ELSEVIER

Teaser Overexpression of nucleolin at the surface of cancer cells and endothelial cells of the tumor vasculature makes it a promising therapeutic target in solid tumors, having been the focus of different therapeutic strategies, including antibodies.

Nucleolin-based targeting strategies for cancer therapy: from targeted drug delivery to cytotoxic ligands

Sofia Romano[1,2,‡], **Nuno Fonseca**[1,3], **Sérgio Simões**[1,4], **João Gonçalves**[5] and **João Nuno Moreira**[1,4]

[1] CNC – Center for Neuroscience and Cell Biology, Faculty of Medicine (Pólo I), University of Coimbra, Rua Larga, 3004-504, Coimbra, Portugal
[2] IIIUC – Institute for Interdisciplinary Research, University of Coimbra, Casa Costa Alemão – Pólo II, Rua Dom Francisco de Lemos, 3030-789 Coimbra, Portugal
[3] TREAT U, SA, Parque Industrial de Taveiro, Lote 44, 3045-508 Coimbra, Portugal
[4] FFUC – Faculty of Pharmacy, University of Coimbra, Pólo das Ciências da Saúde, Azinhaga de Santa Comba, Coimbra, 3000-548 Portugal
[5] iMed. ULisboa - Research Institute for Medicines, Faculty of Pharmacy, University of Lisbon, Avenida Prof. Gama Pinto, 1649-003 Lisbon, Portugal

Cancer is currently the second leading cause of death worldwide and current therapeutic approaches remain ineffective in several cases. Therefore, there is a need to develop more efficacious therapeutic agents, especially for subtypes of cancer lacking targeted therapies. Limited drug penetration into tumors impairs the efficacy of therapies targeting cancer cells. One of the strategies to overcome this problem is targeting the more accessible tumor vasculature via molecules such as nucleolin, which is expressed at the surface of cancer and angiogenic endothelial cells, thus enabling a dual cellular targeting strategy. In this review, we present and discuss nucleolin-based targeting strategies that have been developed for cancer therapy, with a special focus on recent antibody-based approaches.

Novel concepts in cancer therapy

Cancer is currently the second leading cause of death worldwide, only slightly surpassed by heart disease. Estimates relative to 2018 indicate ~18.1 million new cases worldwide and 9.6 million deaths [1]. For several years, therapeutic approaches for the treatment of cancer have comprised surgery, chemotherapy, and radiotherapy, but these are not always effective. In addition, chemotherapy and radiotherapy present severe adverse effects, because they affect not only cancer cells, but also normal tissue. The need for more efficacious therapies that overcome this drawback led to the development of targeted strategies against markers overexpressed in tumors. One example of this kind of therapy is trastuzumab, an antihuman epidermal growth factor

Corresponding author: Moreira, J.N. (jmoreira@ff.uc.pt)
‡ Current address: F-star Biotechnology Ltd., Eddeva B920, Babraham Research Campus, Cambridge CB22 3AT, UK.

Sofia Romano obtained her PhD degree from the University of Coimbra in 2017, under the supervision of Professor João Nuno Moreira and Professor João Gonçalves. Her research involved the generation and *in vitro* characterization of novel antinucleolin antibody formats with cytotoxic activity against cancer cells as well as antibody-dependent cellular cytotoxicity (ADCC) activity. Sofia is currently an associate scientist at F-star Biotechnology Ltd.

João Gonçalves is group leader and member of the board of iMed – Research Institute of Medicines at Faculty of Pharmacy at University of Lisbon, and tenured associate professor, with habilitation at the Faculty of Pharmacy, University of Lisbon. His work on biopharmaceutical development focuses on rational antibody engineering to validate theoretical concepts in autoimmune, inflammatory, cancer, and infectious diseases. The development of better characterization assays and monitoring of antibody therapy in patients, including immunogenicity and pharmacokinetics, also drives his research. He has authored >100 publications in peer-reviewed journals, five book chapters, and five filed patents in Europe, Asia, and USA. He is a co-founder of TechnoAntibodies (a subsidiary of TechnoPhage SA).

João Nuno Moreira is group leader at CNC, University of Coimbra, of the Group on Tumor Microenvironment and Targeted Medicines, and tenured assistant professor, with habilitation, at the Faculty of Pharmacy, University of Coimbra. His scientific activity is focused on targeted drug delivery towards solid tumors. He is ao-author of several publications in peer-reviewed journals, eight book chapters, and nine filed patents (three in the USA and 2 in Europe, and licensed to TREAT U, SA). He has participated, as an invited lecturer, in nine courses on 'Principles and Practice in Drug Development' at MIT (Boston, USA). He is co-founder of TREAT U, SA, a nanotechnology-based spin-off from the UC/CNC.

1359-6446/
https://doi.org/10.1016/j.drudis.2019.06.018

receptor 2 (HER2) antibody, which led to improvements in the long-term outcomes of patients with HER2-overexpressing breast cancer [2]. However, the existence of subtypes of cancer that do not overexpress any of the common markers strongly limits the development of targeted therapies. This is the case of triple-negative breast cancer, which lacks expression of estrogen receptor (ER), progesterone receptor (PR), and HER2 [3,4]. Therefore, it becomes important to identify novel therapeutic targets within these subtypes of cancer, where there are recognized unmet medical needs.

General understanding of tumor development and biology has gone through a major shift with the finding that there is crucial interplay between cancer cells and the surrounding cells and extracellular matrix. Previously regarded as a homogeneous mass of cancer cells, tumors are now recognized as a complex entity, supported by an intricate network of other cells and components, the tumor microenvironment, including endothelial cells, pericytes, fibroblasts, and infiltrating immune cells, as well as cytokines and chemokines. The continuous crosstalk between cancer cells and the tumor microenvironment favors tumor development, enhancing its proliferation and metastasization [5–7].

The tumor microenvironment is now considered an important target for cancer therapy. On the one hand, because stromal cells do not present the same proliferative potential as cancer cells, they are less likely to evolve and become resistant to therapy [8,9]. On the other hand, the increased tumor interstitial pressure, to which the tumor microenvironment contributes, renders drug transport and accumulation in the tumor more difficult. The development of a vasculature to support the tumor has been described as one of the hallmarks of cancer, because it supplies the nutrients and oxygen required, as well as the elimination of metabolic wastes and carbon dioxide [5]. Therefore, antiangiogenic therapies have been a focus of research and some inhibitors of angiogenesis are currently used, including the antivascular endothelial growth factor (VEGF) antibody bevacizumab, which is used as monotherapy (in multiform glioblastoma) or in combination with chemotherapy or cytokine therapy (in colorectal cancer, metastatic breast cancer, non-small cell lung cancer, and metastatic renal cell carcinoma) [10,11].

Therapies that target both cancer cells and the surrounding microenvironment are now envisioned as a way to more effectively achieve relevant anticancer effects, given that remaining cancer cells would not have an appropriate environment in which to further grow and proliferate [12,13].

In this review, we describe the therapeutic strategies devised against nucleolin, a protein present at the surface of tumor cells, including cancer cells and tumor vasculature, therefore allowing targeting of different cellular compartments of a solid tumor, by means of a single molecule. Special focus is given to recently developed antinucleolin antibody-based therapeutic approaches.

Cell surface nucleolin: targeting opportunity towards tumors of diverse histological origins

Nucleolin is a 76-kDa protein that was first described as a nucleolar protein in Novikoff hepatoma cells and Chinese Hamster Ovary (CHO) cells [14,15]. Its expression was later reported to broadly occur in all cells in a proliferation-dependent manner [16]. It has a tripartite structure, encompassing: a N-terminal domain with acidic stretches, involved in several protein–protein interactions, which controls rDNA transcription; a central globular domain, with four RNA-binding domains (RBDs), involved in pre-RNA processing; and a C-terminal domain, comprising arginine-glycine-glycine repeats, which interacts with ribosomal proteins. Nucleolin is a nonhistone phosphoprotein and can represent up to 10% of total nucleolar protein in exponentially growing eukaryotic cells. In the nucleus, its main functions include regulation of rRNA synthesis and ribosome biogenesis. Nucleolin acts as a shuttling protein between the cytoplasm and the nucleus, and promotes the import of ribosomal subunits to the nucleus, where it brings them together with RNA [17–19].

Nucleolin at the cell surface

In highly proliferating cells, such as metabolically active cancer cells, the mechanism underlying nucleolin translocation from the nucleus to the cytoplasm and cell membrane, although not completely clear, relies on an unconventional vesicular secretory pathway that is independent of the endoplasmic reticulum (ER)–Golgi complex [20]. At the membrane, nucleolin forms clusters in an actin cytoskeleton-dependent manner [20]. This translocation also occurs in endothelial cells of angiogenic blood vessels [21]. In fact, in angiogenic endothelial cells, surface translocation of nucleolin is mediated by heat shock cognate 70 (HSc70) upon stabilization of its interaction with actin-based myosin heavy chain 9 (MyH9) [22], a linker between nucleolin and cytoskeleton [23]. Nevertheless, nucleolin phosphorylation status [24] and glycosylation [22] have been described to heavily influence its cellular compartmentalization, although other modulators of the process described above cannot be ruled out.

Expression of surface nucleolin has also been identified in cancer stem cells (CSCs) from different breast cancer cells lines, correlating with tumorigenic potential [25]. Given that CSCs are highly tumorigenic, with a crucial role in mediatization and tumor relapse [26,27], these findings further highlight the relevance of nucleolin as a therapeutic target. The association of nucleolin with the stemness phenotype and its implications for multicellular targeting have been recently reviewed by Fonseca *et al.* [28].

Importantly, nucleolin overexpression, namely at the cell surface, is restricted to tumor cells, whereas major organs, such as heart, lungs, liver, or spleen, and the respective vasculature, lack cell surface nucleolin [23,29,30]. Furthermore, the nucleolin-binding F3 peptide binds to bone marrow endothelial progenitor cells [31], which suggests that these cells express surface nucleolin. This is further supported by the nucleolin-promoted execution of the hematopoietic stem cell gene expression program by human/stem progenitor cells [32]. However, antinucleolin agents have not shown significant effects on white blood cell count [33,34].

Notwithstanding those observations, deregulated expression of nucleolin has been associated with higher risk of recurrence or poorer overall survival for several cancers (reviewed in Ref. [35]), defining the potential of nucleolin as both a prognostic marker and a therapeutic target, with recognized interplay across cancer biology.

The multiple roles of nucleolin

Although the role of nucleolin at the cell surface is still not fully understood, different studies have revealed interactions with different proteins and signaling pathways (Fig. 1). At the cell surface, nucleolin can bind to, and mediate the internalization of, a

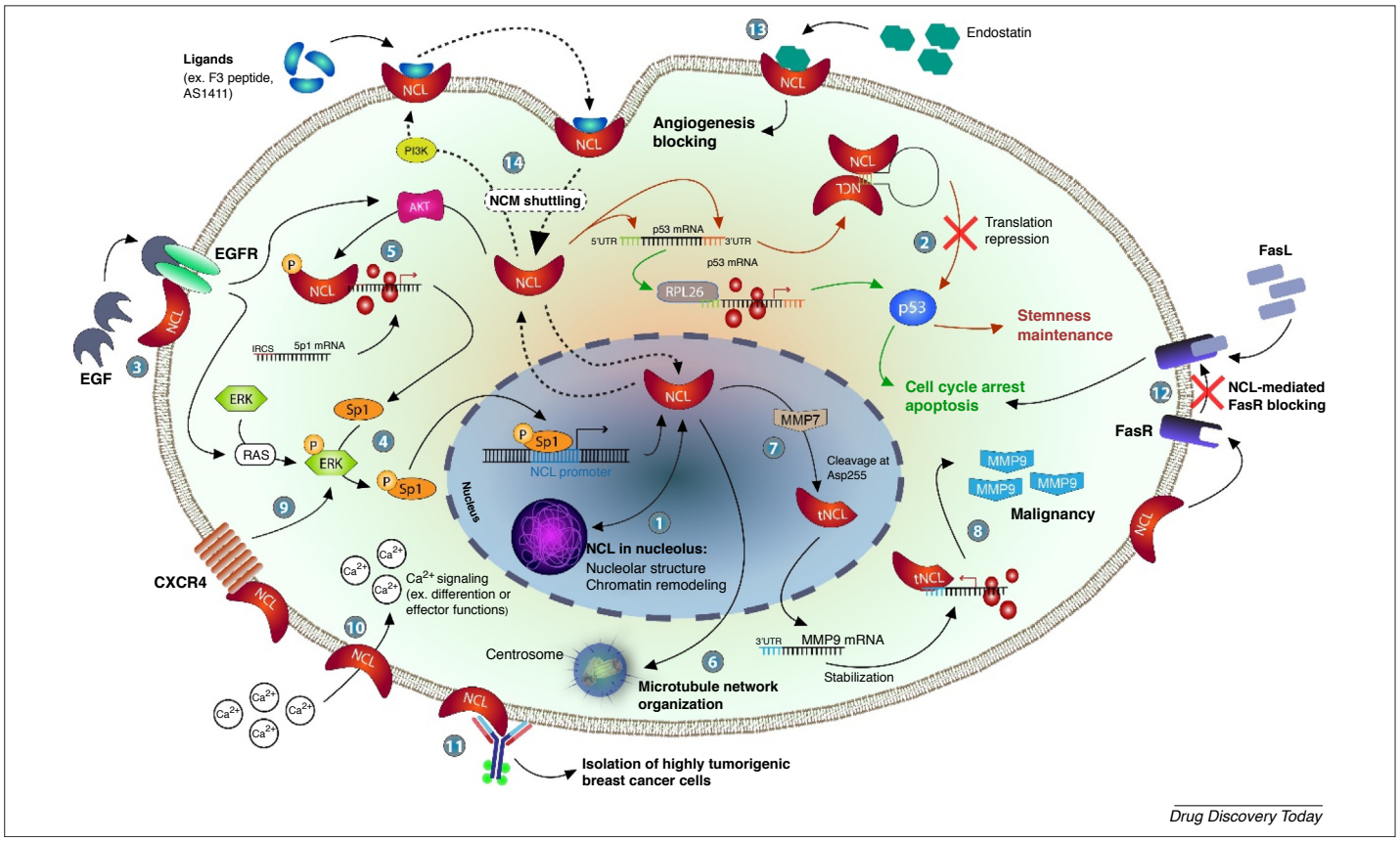

FIGURE 1

The multiples roles of nucleolin (NCL). Chromatin remodeling (**1**) or the maintenance of embryonic stem cells through blocking p53 expression (**2**) are among some of the physiological functions of NCL. In some cancer cells, besides interacting with epidermal growth factor receptor (EGFR) (**3**), NCL overexpression depends on EGFR-mediated Sp1 transcription factor activation (**4**). It further stabilizes and modulates Sp1 translation, thus closing a positive feedback loop (**5**). Besides supporting the organization of microtubules at centrosomes (**6**), NCL can be truncated by matrix metalloproteinase (MMP)-7 (**7**), further supporting MMP9-mediated malignant transformation (**8**). At the cell surface, NCL interacts with C-X-C motif chemokine receptor 4 (CXCR4) leading to the activation of extracellular signal-regulated kinase (ERK) (**9**). Furthermore, cell surface NCL mediates calcium internalization (**10**) and can be used for the selection of highly tumorigenic cancer cells (**11**). Although NCL blocks Fas receptor (FasR), preventing apoptosis signaling (**12**), it also mediates the antiangiogenic activity of ligands, such as endostatin (**13**). Finally, cell surface NCL mediates the internalization and nuclear localization of different ligands through continuous shuttling between the cell membrane and the nucleus (**14**). Abbreviations: EGF, epidermal growth factor; FasL, Fas ligand; NCM, nucleus–cytoplasm–membrane shuttling; RPL26, ribosomal protein L26; tNCL, truncated NCL.

plethora of ligands in a calcium-dependent manner [36]. These include urokinase-type plasminogen activator (involved in cell proliferation and migration during angiogenesis) [37], the HIV inhibitors midkine [38] and pleiotrophin [39], and the cell proliferation inhibitor lactoferrin [40]. Upon binding to nucleolin, the complex thus formed is quickly internalized and transported to either the cytoplasm or the nucleus [20,29,36,40]. Nucleolin also binds to endostatin, an endogenous 20-kDa protein with antiangiogenic and antitumoral effects that has low toxicity. Shi *et al.* identified nucleolin as being responsible for the internalization of endostatin and its transport to the nucleus of endothelial cells, leading to antitumoral and antiangiogenic effects [29,30].

At the cell surface, nucleolin interacts with epidermal growth factor receptor (EGFR) and Ras, promoting EGFR phosphorylation and dimerization and contributing to anchorage-independent cell growth in cell lines of diverse histological origin, such as breast, kidney, and brain [41,42]. Expression of nucleolin, Ras, or EGFR in the MDCK cell line did not alter the colony formation capacity of the cells. However, *in vivo*, the overexpression of these three proteins enabled a higher rate of tumor growth than cells expressing just one or two of those proteins [42]. The potential of these proteins as therapeutic targets has been supported in several studies. Incubation of prostate and colon cancer cell lines with a Ras inhibitor and a nucleolin inhibitor, resulted in increased cell death and inhibition of anchorage-independent cell growth and cell migration, relative to single drug incubations [43]. Incubation of U87-MG glioblastoma cells with the same combination of inhibitors led to higher cell death and reduced cell migration [44]. However, in an ectopic U87-MG-derived animal model, administration of both inhibitors resulted in similar tumor growth inhibition as single drug treatment. Nevertheless, inhibition of cell proliferation and cell death was more pronounced in tumors treated with the drug combination, as evaluated by Ki-67 and caspase 3 staining [44].

Nucleolin also interacts with the other receptor tyrosine kinases of the ErbB family, including HER2. This interaction promotes cell growth, as suggested by the increased colony formation and anchorage-independent growth of cells observed upon nucleolin and HER2 overexpression. In addition, nucleolin promoted HER2 phosphorylation and subsequent activation of the mitogen-acti-

vated protein kinase/extracellular signal-regulated kinase (MAPK/Erk) pathway. Accordingly, nucleolin inhibition in a HER2-positive cell line led to decreased HER2 activation and decreased cell viability [45]. Similarly to what had been described for nucleolin and EGFR, combined treatment with nucleolin and HER2 inhibitors revealed superior efficacy compared with single treatments in terms of cell viability, anchorage-independent growth, and the invasion capacity of breast cancer cells [46].

In nonHodgkin's lymphoma, surface nucleolin forms a complex with Fas, a member of the tumor necrosis factor (TNF) superfamily of apoptosis receptors. The interaction blocks the binding of Fas to its ligand, FasL, resulting in a decrease in the apoptosis level. This suggests that nucleolin has a role in cells that, although overexpressing Fas, are resistant to its activation [47].

Nucleolin interaction with members of the family of heparin-bound growth factors has also been described. In prostate cancer cells, it interacts with hepatocyte growth factor (HGF), a regulator of carcinoma growth and invasion that binds to the Met receptor. In the absence of the latter, HGF is still able to activate the protein kinase ERK and Akt signaling pathway upon binding to nucleolin [48]. In hepatoma cells, nucleolin interacts with hepatoma-derived growth factor (HDGF), involved in cell proliferation and metastasis. HDGF elicits translocation of nucleolin to the cell surface, where the two proteins interact and, similarly to that observed with HGF, activate the Akt pathway [49].

In papillary thyroid cancer and glioblastoma, nucleolin activates C-X-C chemokine receptor 4 (CXCR4) signaling, contributing to cell growth, migration, and invasion. Knockdown of nucleolin using small interfering RNA (siRNA) led to decreased ERK and Akt phosphorylation, resulting in impairment of overall cell growth and migration [50–52]. In addition, in glioblastoma, nucleolin interacts with the $\alpha_v\beta_3$ integrin and receptor protein tyrosine phosphatase β/ζ (RPTPβ/ζ), components of the phosphoinositide 3-kinase (PI3K)/Akt pathway [53]. In this study, surface nucleolin was detected only in cells expressing $\alpha_v\beta_3$ integrin and was dependent on integrin phosphorylation upon RPTPβ/ζ activation [53].

In leukemia CEM cells, nucleolin has been described to be present at the cell surface in a complex of 500 kDa comprising several proteins: Wnt-related protein A and B, which are involved in cell proliferation and differentiation; Ku80, which promotes adhesion and invasion of tumor cells; signal recognition particle 68 and 72 (SRP68 and SRP72), from the ribonucleoprotein complex; gC1q-R, a regulator of cell adhesion, migration, and invasion; and ribosomal proteins S4 and S6 [54]. However, the relevance of the existence of nucleolin in this complex, and its presence in other cell types, remains to be clarified.

Overall, the aforementioned examples support the involvement of surface nucleolin in several pathways that regulate tumor growth and mediatization, thus representing an opportunity that should be explored in terms of drug targeting. In fact, different attempts have been performed, based either on exploiting nucleolin as a target protein for the intracellular delivery of therapeutic payloads or on the disruption nucleolin intracellular signaling. As described in the following sections, different antinucleolin agents present different therapeutic effects. Although the reasons for these differences remain unexplored, different nucleolin domains are targeted by these agents, which could account for these different effects.

Therapeutic strategies exploiting nucleolin-based targeting

Surface nucleolin as a target for intracellular drug delivery

Among the different nucleolin-binding ligands that have been tested so far, the F3 peptide and the AS1411 aptamer are those that have been explored the most.

F3 peptide as targeting ligand for intracellular drug delivery

The nucleolin-binding F3 peptide is a 31-amino acid peptide that has been generated by phage display, from a cDNA library obtained from mRNA of human and mouse tissues, which included bone marrow, spleen, and malignant tissues [31]. It was further demonstrated that binding to both cancer cells and tumor vasculature in murine models of cancer was nucleolin mediated. F3 peptide binding to nucleolin appears to occur at the N-terminal domain of the latter, because the antibody NCL3, generated against a region of this domain, inhibited F3 peptide internalization into nucleolin-expressing cells [21]. These properties potentiated the assessment of this peptide as a targeting ligand of nanoparticles (NPs) containing chemotherapeutic drugs (doxorubicin [55] or cisplatin [56]), photodynamic therapy (PDT) agents [57] or chemically conjugated to radiotherapeutics [58] (Table 1). In this respect, NPs of different nature have been tested in different types of cancer model.

A F3 peptide-targeted cisplatin-loaded hydrogel NP affected, upon intravenous (i.v.) administration, the tumor vasculature, as suggested by the reduced viability of primary tumor endothelial cells and vascular density of a teratoma model with a human vasculature. This resulted in decreased tumor progression, relative to treatment with combined administration of free cisplatin and empty targeted NPs. Moreover, in A2780- or SKOV3-derived tumors (cisplatin-sensitive and cisplatin-resistant, respectively) it reduced tumor volume, in contrast to the aforementioned controls, resulting in improved survival [56].

F3 peptide-targeted strategies also improved the outcome of photofrin-containing NPs [57] and ^{213}Bi-DTPA-based radiotherapy [58], namely in terms of survival in *in vivo* models of gliosarcoma and peritoneal carcinomatosis, respectively.

The potential of intracellular drug delivery mediated by nucleolin has been further confirmed in different settings. Treatment of mice bearing MDA-MB-435 tumors in the mammary fat pad, with F3 peptide-targeted pH-sensitive liposomes containing doxorubicin, suppressed tumor invasion into adjacent healthy tissues, in contrast to several different controls tested, including the non-targeted counterparts [55]. The versatility of the strategy was further demonstrated with the encapsulation of a drug combination of doxorubicin and the sphingolipid, C6-ceramide (inhibitor of the PI3K pathway) [59]. A killing level of 100% was achieved against both stem-like and non-stem MDA-MB-231 triple-negative breast cancer cells, in contrast to the targeted counterpart containing doxorubicin alone, which did not go beyond 90% [25]. The versatility of the strategy has also been reflected by the nature of the drug to be encapsulated [60]. Non-immunogenic [61] F3 peptide-targeted liposomes containing anti-polo-like kinase 1 (*PLK1*) siRNA decreased viability of both PC-3 prostate cancer cells and HMEC-1 endothelial cells, a model of endothelial cells from angiogenic blood vessels. In addition, upon combination with paclitaxel, a threefold reduction in IC_{50} (relative to paclitaxel alone) was achieved [62].

TABLE 1

F3 peptide-based agents for intracellular drug delivery

Drug and delivery agent	*In vitro* effects	*In vivo* model	Schedule	*In vivo* effects	Refs
CIS-loaded, hydrogel NPs	↓ Viability of TEC[a] (1 μg/ml, 72 h)	*BD/T*: C57BL6 mice 10^7 ID8-VEGF cells Ectopic (flank)	*BD*: i.v. 100 mg/kg F3-FITC-NP	High uptake in tumor vessels No significant uptake in liver and kidney	[56]
		T: Nude mice 10^7 SKOV3 or A2780 Ectopic (axillary) 2×10^6 ID8 cells Ectopic (i.p. injection)	*T*: i.v. 100 mg/kg F3-CIS-NP (days 10, 14, and 21)	↓ Tumor weight (2.5-fold)[b] ↓ Tumor volume (3.5-fold)[a] ↑ Regions of hemorrhage and necrosis[a] ↓ Tumor islet size[a]	
		T: Teratoma model Nonobese SCID mice 10^6 undifferentiated H9 embryonic stem cells Ectopic (axillary) 10^5 HEY1 cells within teratoma	i.v. 100 mg/kg F3-CIS-NP (days 10 and 14; ID8 and SKOV3 xenografts also day 21) i.v. F3-Cis-Np (75 mg/kg CIS) (days 10, 14, 17, and 21)	↓ tumor volume[a] ID8: ↑ survival[a] ↓ Tumor progression[a] ↓ Tumor weight[a] ↓ Tumor blood vessels[a]	
Photofrin-loaded PEG-PLGA NPs	↓ Viability of MDA-MB-435 (90%) (10 mM, 4 h)	Fisher 344 rats 10^5 Rat 9 L cells Orthotopic	*I*: i.v., 200 mg NP/kg	↑ Half-life (threefold) ↑ Contrast-to-noise ratio (twofold)	[57]
			T: i.v. of F3-targeted photofrin/iron oxide-encapsulated NPs with light activation 1 h later	↑ Survival (2.5-fold)	
^{213}Bi-DTPA-$[F3]_2$	↓ Clonogenic capacity ID50 − 23.9 to 119 kBq/ml (EMT6, MIAPACA, CMT93, OVCAR3 and MDA-MB-435)	SCID mice 10^7 MDA-MB435 (peritoneal carcinomatosis model) Orthotopic (i.p.)	*BD*: i.p. 3.7 MBq ^{68}Ga-DTPA-$[F3]_2$ *T*: i.p., 1.85 MBq ^{213}Bi-DTPA-$[F3]_2$, between days 4 and 14 (tumor prevention) or between days 16 and 26 (tumor reduction)	Accumulation in tumor (32%) and kidney ↑ Survival (80% or 62.5%, respectively) Smaller number of tumor nodules	[58]
Anti-*PLK1* siRNA-loaded pH-sensitive LPs	↓ Viability (2 mM siRNA, 80 h)[b] PC3: 57% HMEC: 39.4%	–	–	–	[62]
DOX-loaded pH-sensitive LPs	IC_{50} (24 h), untargeted and targeted: MDA-MB-435S: 87.33 and 3.95 mM HMEC-1: 3.57 and 0.195 mM ↓ Vessel formation (27.5%)	Balb/c mice MDA-MB-435S Orthotopic	*BD*: i.v., 0.5 μmol phospholipid/mouse	↑ Accumulation in tumors (57-fold) ↓ Accumulation in spleen and liver	[25,55]
			T: i.v., 5 mg DXR/kg, every week for 5 weeks	↓ Viable rim area ↑ Cell death in tumor periphery ↑ Tumor necrosis ↓ Vascular density ↓ Invasion of adjacent tissue	
F3-Gel, 2F3-Gel, and 3F3-Gel fusion toxins (comprising 1–3 repeats of F3 peptide sequence, respectively)	↓ Viability, IC_{50} (48 h), untargeted and targeted (monomeric, dimeric, and trimeric F3): LNCaP: 4100, 470, 63, and 88 nM PC3: 4200, 360, 99, and 94 nM DU145: 3100, 310, 73, and 100 nM	*BD*: Athymic mice 2×10^8 LNCaP Ectopic (left flank)	*BD*: i.v., 8 mg/kg Gel	↑ Accumulation in tumors (3.6- and 3.1-fold for 2F3-Gel and 3F3-Gel, respectively)	[63]
		T: Athymic mice 2×10^8 U87 MG Ectopic (left flank)	*T*: i.v., 8 mg/kg Gel (days 9, 12, and 15)	↓ Tumor volume (44% or 39% for 2F3-Gel and 3F3-Gel, respectively)	

BD, biodistribution studies; ^{213}Bi-DTPA, alpha emitter ^{213}Bi, conjugated to diethylenetriaminepentaacetic acid; CIS, cisplatin; DOX, doxorubicin; Gel, gelonin; *I*, imaging studies; LP, liposome; *T*, therapeutic studies. Cells: 9 L, rat gliosarcoma; A2780, HEY-1, OVCAR3 and SKOV3, human ovarian cancer; CMT93, murine colon cancer; DU145, LNCaP and PC3, human prostate cancer; EMT6, MDA-MB-231, human breast cancer; HMEC-1 and TEC, human tumor endothelial cells; ID8, murine ovarian tumor; MIAPACA, human pancreatic cancer; U87 MG, human glioblastoma. Unless otherwise indicated, percentages indicated are in comparison to the control without the F3 peptide.

[a] Relative to CIS + F3-NP.

[b] Relative to untreated cells.

A targeting approach based on fusion toxins, comprising the F3 peptide and the ribosome-inactivating protein gelonin, has also been developed. Three formats of fusion toxins, differing in the number of F3 peptide sequences used, presented improved cytotoxicity against prostate cancer cell lines, relative to gelonin alone. However, only the multimeric formats enabled improved tumor accumulation and reduced tumor growth in ectopic models of prostate cancer and glioblastoma, respectively. The most potent effects obtained with these formats, relative to the monomeric fusion toxin, could be the result of their multivalency and/or improved exposure of the F3 peptide sequences, enabled by the use of multimers and the linker $(GGSG)_3$ between each F3 peptide sequence [63].

AS1411 aptamer as a targeting ligand for intracellular drug delivery

Aptamers are guanine-rich oligonucleotide molecules that form four-stranded structures and present specific protein-binding (aptameric) properties. One of the main issues regarding oligonucleotide-based therapies is their stability in serum and in the presence of cellular nucleases. However, aptamers present increased resistance to nuclease activity, because of their quadruplex structure, making them more suitable for therapeutic purposes.

The AS1411 aptamer, which binds to RNA-binding domains of nucleolin [64], has been used to target NPs of different natures, containing either siRNA [65] or small drugs [66–70] towards nucleolin-overexpressing cells (Table 2). Similar to what has been described for the F3 peptide, AS1411-based strategies led to improved cytotoxicity against nucleolin-overexpressing cell lines relative to nontargeted counterparts [71–73]. Similar effects to those reported for F3 peptide-targeted approaches were also observed, namely marked tumor growth inhibition and improved survival, depending on the tumor model.

A different targeting approach has been recently developed, comprising an aptamer–drug conjugate. Li *et al.* synthesized an AS1411-paclitaxel conjugate, in which those components were bridged by a cathepsin B-sensitive dipeptide, which was revealed to be stable in the blood. Upon endocytosis, cathepsin B cleaved the linker, rendering paclitaxel active and leading to decreased cell viability of nucleolin-overexpressing cell lines by blocking cell cycle in G2/M phase. The targeting efficacy of AS1411 was confirmed by its higher accumulation in tumors and lower accumulation in liver and kidney relative to a control aptamer-paclitaxel conjugate. Importantly, in an *in vivo* model of ovarian cancer, this strategy not only proved to be more efficacious in decreasing tumor volume than administration of free paclitaxel, but also presented less systemic toxicity. In contrast to paclitaxel, treatment with the conjugate did not lead to weight loss or change over time, and had a decreased effect on white blood cell count, while also presenting less toxicity in several organs [34].

Recently, the targeting properties of AS1411 have also been exploited for the delivery of a thrombin-loaded DNA nanorobot [74]. This comprised a DNA origami, functionalized on the surface by AS1411 and loaded with thrombin. Opening of the DNA structure and release of the payload was the result of specific binding of the coupled AS1411 to nucleolin-overexpressing human umbilical vein endothelial cells (HUVEC). In an *in vivo* breast cancer model, the nanorobots accumulated in the tumor more efficiently than the nontargeted counterparts and colocalized with CD34, confirming their association with the tumor vasculature. Thrombosis was observed in all tumor blood vessels (but not in healthy organs), as well as tumor necrosis, after administration of the AS1411-decorated thrombin-loaded nanorobot, in contrast to the nontargeted or empty controls. The nanorobot resulted in improved survival in several mouse models, especially those with a high grade of tumor vascularization. This was the first AS1411-based approach to report effects at the tumor vasculature level. Importantly, *in vivo* safety of the nanorobot was confirmed in healthy Bama minipigs. Intravenous administration of the nanorobot did not affect blood coagulation and did not induce thrombosis in major organs [74].

AS1411 has also been revealed to have antiproliferative activity on its own. At the molecular level, following incubation with breast cancer cells, it enabled destabilization of B cell lymphoma 2 *(bcl-2)* mRNA and downregulated expression levels of miR-21, miR-221, miR-222, and miR-103, usually associated with tumor aggressiveness and resistance to antineoplastic therapy [75,76]. Furthermore, inhibition of nuclear factor kappa B (NF-κB) activation was observed following incubation with human prostate, breast, and lung cancer cell lines [77]. The pharmacological activity, both *in vitro* and i*n vivo*, that the AS1411 aptamer has revealed against tumors of diverse histological origin, including leukemia [78], supported a Phase II clinical trial in patients with acute myeloid leukemia, in combination with cytarabine (NCT00512083). Improved antileukemic activity, with an acceptable safety profile and improved overall survival, was observed. However, a Phase IIb clinical trial to determine duration of response and survival (NCT01034410) was terminated. No reports on new clinical trials have since been disclosed.

Notably, the positive outcome that has been observed with both F3 peptide- and AS1411-targeted platforms in tumor models from diverse histological origins, supports nucleolin as a relevant therapeutic target in a range of tumors.

Nucleolin as a target for pseudopeptides and antibody formats

Although the effectiveness of AS1411 in clinical trials remains unconfirmed, the promising results obtained in several models of nucleolin-overexpression tumors paved the way to the development of other entities aiming at disrupting nucleolin signaling, namely pseudopeptides (Table 3) and antibody formats (Table 4).

Anti-nucleolin pseudopeptides

The nucleolin-binding pseudopeptide HB-19 has a pentavalent structure comprising the tripeptide lysine-glycine-proline (with a reduced bond between the lysine and proline residues) coupled to an 8-amino acid template. The reduced bond between lysine and proline provides resistance to serum proteases [79]. Upon binding to the C-terminal domain of nucleolin [80], this pseudopeptide is translocated to the cytoplasm, but not to the nucleus, leading to a reduction in nucleolin levels both at the cell surface and in the cytoplasm [81].

HB-19 decreased the colony-formation capacity of several cell lines and the proliferation and migration of VEGF-stimulated HUVEC, and resulted in antiangiogenic effects in a chick chorioallantoic membrane (CAM) assay, reducing blood vessel length by 50%. Importantly, these effects translated into antitumoral and antiangiogenic effects in *in vivo* breast cancer models, without evidences of toxicity in normal tissues [81]. HB-19 activity relied on the decrease of both the percentage of cells in the S phase of the cell cycle and ERK1/2 phosphorylation [81]. The activity of HB-19 has been

TABLE 2

AS1411-based agents for intracellular drug delivery

Drug and delivery agent	*In vitro* effects	*In vivo* model	Schedule	*In vivo* effects	Refs
PTX-loaded PEG-PLGA NPs	↓ Viability of C6 IC_{50}, 96 h: Untargeted: 0.08 μg/ml (94 nM) Targeted: 0.03 μg/ml (35 nM)	Nude mice 2×10^6 C6 cells Ectopic (right anterior limb) Wistar rats 3×10^7 C6 cells Orthotopic	*BD*: i.v., 3 mg/kg PTX *T*: i.v., 3 mg/kg PTX, (days 6, 8, 10, 12, 14, 16, and 18) i.v., 3 mg/kg PTX, (days 4, 6, 8, 10, 12, and 14)	↑ Accumulation in tumor ↓ Tumor volume and weight ↑ Survival (22%)	[66]
DOX-loaded nanorods	↓ Viability of MCF-7 (50%) (40 mM, 48 h)	–	–	–	[67]
PTX-loaded, PLGA-lecithin-PEG NPs	↓ viability of MCF-7 and GI-1 (100 μg/ml, 117 mM)	–	–	–	[126]
DTX-loaded, TGN-conjugated PEG-PCL NPs	–	Balb/c mice 5×10^5 C6 cells Orthotopic	*I*: i.v. *T*: i.v., 6 mg/kg DTX (every 3 days, 3 times/day)	↑ Ratio tumor:brain accumulation ↑ Survival (increase of 47% or 28% for AS1411/TGN- or AS1411-targeted NPs, respectively)	[71]
PTX-loaded protein NPs	↓ Viability of MCF-7 (50 μg/ml, 59 mM)	–	–	–	[68]
NMM-loaded gold NPs	↓ Viability of HeLa (30%) (10 nM NP, 24 h)	–	–	–	[70]
Anti-BRAF siRNA-loaded, MAL-activated PEG-DOPE LPs	↓ Viability of A375 (30 nM, 48 h)	Balb/c nude mice 2×10^6 A357 cells Ectopic (right flank)	*BD*: i.v., 1.2 mg Cy5.5-siRNA /kg *T*: i.v., 1.2 mg/kg siRNA, 3 consecutive days	Accumulation in tumor and kidneys Gene silencing in tumor tissues ↓ Tumor cell number Tumor necrosis	[65]
DOX- or AZD8055-loaded gold NPs	↓ Viability of MCF-7, OMM1.3, Mel202 (72 h) DOX: 49.4, 58.1 and 38.5% AZD8055:17.9, 21.6 and 34.5%	–	–	–	[69]
PTX-loaded, pH-sensitive micelles	↓ Viability of SKOV3 IC_{50} (pH 7.4, 48 h): untargeted, 0.832 mM; targeted, 0.552 mM IC_{50} (pH 5.8, 48 h): untargeted, 0.298 mM; targeted, 0.108 mM	–	–	–	[33]
DOX-loaded, MAL-PEG-LPs	↓ viability of MCF-7/ADR	Nude mice 5×10^6 MCF-7/ADR cells Ectopic (left flank)	i.v. 0.2 mg/kg (DOX), every 4 days, 4 times/day (tumor site heated to 42 °C)	↑ Accumulation in tumor ↓ Tumor volume	[127]
DOX-loaded, redox-responsive HPAEG	↓ Viability of MCF-7 IC_{50} (48 h): non-targeted, 2.30 mg/ml (4.23 mM); targeted, 1.33 mg/ml (2.45 mM)	–	–	–	[128]
Gemcitabine-loaded PEG-PLGA NPs	↓ Viability of A549 IC_{50} (48 h): untargeted, 28.9 mg/ml (110 mM); targeted, 4.9 mg/ml (19 mM)	–	–	–	[129]
DTX-loaded polymeric NP	↓ viability of LNCaP IC_{50} (48 h): untargeted, 0.251 mg/ml (311 nM); targeted, 0.085 mg/ml (105 nM)	Balb/c mice 2×10^7 LNCaP cells Ectopic (right flank)	i.v. 10 mg/kg of DTX, every other day, for 2 weeks	↓ Tumor weight (35%)	[130]
DOX-loaded, PEP polymersome	↓ Viability of MCF-7 IC_{50} (48 h): control aptamer, 369.4 ng/mL (680 nM); targeted, 210.9 ng/ml (388 nM)	Mice bearing MCF-7 tumors	*BD*: i.v. 2 mg/kg of ICG Cellular uptake: i.v. 5 mg/kg DOX *T*: i.v. 5 mg/kg DOX (days 0, 3, and 6)	↑ Accumulation in tumor (1.75-fold)[a] ↑ Cellular uptake (twofold)[a] ↓ Tumor volume (45%)[a] ↑ Tumor growth inhibition (43%)[a] ↑ Apoptotic area[a] ↓ Cell proliferation[a]	[72]

TABLE 2 (*Continued*)

Drug and delivery agent	*In vitro* effects	*In vivo* model	Schedule	*In vivo* effects	Refs
DTX-loaded, PLGA-TPGS NPs	↓ Viability, IC_{50} (48 h), untargeted and targeted: MCF-7: 6.88 and 1.69 mg/ml (8.52 and 2.09 mM) HeLa: 3.07 and 0.47 mg/ml (3.8 and 0.58 mM)	SCID mice 2×10^6 MCF-7 cells Ectopic (back)	*BD*: i.v. 1 mg/kg IR-780	↑ Accumulation in tumor	[131,132]
		TA2 mice (spontaneous breast cancer)	*T*: i.v. 10 mg/kg DOX (days 0, 4, 8, 12, and 16)	↓ Tumor volume	
		SCID mice 2×10^6 HeLa cells Ectopic (back)	*T*: i.v. 10 mg/kg DOX (days 0, 4, 8, 12, and 16)	↑ Survival (22%)	
			T: i.v. 10 mg/kg DOX (days 0, 4, 8, 12, 16, and 20)	↑ Survival (24%)	
PTX-loaded, PGG NPs	↓ Viability, IC_{50} (48 h), untargeted and targeted: U87 MG: 0.73 and 0.21 mM	Balb/c mice 5×10^5 U87 MG cells Orthotopic (right striatum)	*I:* i.v. DiR-labeled AS1411-PGG-PTX (10 mg DiR)	↑ Accumulation in brain ↑ Penetration in glioma tissue	[73]
			T: i.v. 10 mg/kg PTX (days 3, 6, 9, and 12)	↑ Survival (1.1 fold)	
CPT-loaded, pegylated PAMAM	↓ Viability, IC_{50} (48 h), untargeted and targeted: HT29: 5.75 and 2.07 mg/ml (16.5 and 6 mM) C26: 2.67 and 0.67 mg/ml (7.66 and 1.92 mM)	Balb/c mice 3×10^5 C26 cells Ectopic (right flank)	i.v. 3 mg/kg CPT (twice a week, for 3 weeks)	↓ Tumor volume ↑ Survival	[133]
let-7 miRNA gene-loaded EVs	–	Balb/c mice 3×10^6 MDA-MB-231 cells Ectopic (right flank)	*I:* i.v., 50 mg EV *T*: i.v. 150 mg let-7, every other day, until day 25	↑ Accumulation in tumor ↓ Tumor volume (29%)	[134]
DOX/SPION-loaded, PLGA NPs	↓ Viability, IC_{50} (48 h), untargeted and targeted: C26: 1.76 and 0.37 mg/ml (3.24 and 0.68 mM)	Balb/c mice 3×10^5 C26 cells Ectopic (right flank)	i.v. 10 mg NP/kg	*BD*: ↑ accumulation in tumor *T*: ↑ survival (1.2-fold) ↑ Tumor growth delay (1.4-fold)	[135]
DOX-loaded, PEG-PAE micelles	↓ Viability of MCF-7	–	–	–	[136]
AS1411-PTX conjugate	↓ Viability, IC_{50} (72 h), untargeted and targeted[a] SKOV3: 24.4 and 7.6 nM OVCAR3: 21.7 and 9.8 nM	Balb/c mice 2×10^6 SKOV3 cells Ectopic (left armpit)	*BD*: i.v. 5 mg/kg nanoconjugate-rhodamine B, single dose	*BD*: ↑ accumulation in tumor[a] ↓ Accumulation in liver and kidney[a]	[34]
			T: i.v. 2.4 mmol/kg (twice a week, for 4 weeks)	*T*: ↓ tumor volume[a] ↓ Cell proliferation[a]	
Thrombin-loaded nanorobot	Blood coagulation	Nude mice 2×10^6 MDA-MB-231 cells and Matrigel Orthotopic	*I:* i.v. Cy5.5-nanorobot	*I:* ↑ accumulation in tumor (sevenfold)[b] Presence of dense thrombi in all tumor vessels	[74]
		C57BL/6 J mice 5×10^6 B16-F10 Right flank	*T*: i.v. 1.5 U accumulated thrombin/mouse, every 3 days, 6 treatments	*T*: ↓ tumor volume[c] ↑ Survival (1.3 fold)[c]	
		Nude mice SKOV3 cells Ectopic	*T*: i.v. every other day, 14 days	*T*: ↓ tumor volume[c] (37.5% of mice with complete tumor regression) ↑ Survival (2.2 fold)[c]	
			T: i.v. 1.5 U accumulated thrombin/mouse, every 3 days, 6 treatments	*T*: ↓ tumor volume[c] ↑ survival[c]	
AS1411	↓ Viability of cell lines of 14 histological origins, most with reduced viability of at least 30% (for 6.3 mM)	Nude mice DU145 Ectopic	i.p. 5 mg/kg (days 1, 2, 3, 5, 7, and 9)	↓ Tumor growth	[78]
		Nude mice A549 SKMES	i.v. 5–40 mg/kg (days 1–5, daily)	A549: ↓ tumor size SKMES: ↓ tumor volume	

BD, biodistribution studies; CPT, camptothecin; DOPE, dioleoylphosphatidylethanolamine; DOX, doxorubicin; DTX, docetaxel; EV, extracellular vesicles; HPAEG, hyperbranched poly(2-((2-(acryloyloxy)ethyl)disulfanyl)ethyl 4-cyano-4-(((propylthio)carbonothioyl)-thio)-pentanoate-co-poly(ethylene glycol) methacrylate); *I*, imaging studies; MAL, maleimide; NMM, *N*-methylmesoporphyrin IX; PAA, polyacrylamide; PAE, poly(β-amino ester); PAMAM, polyamidoamine dendrimer; PEG, polyethylene glycol; PEP, poly[methoxy-poly(ethylene glycol)/ethyl-p-aminobenzoate phosphazene; PCL, polycaprolactone; PGG, poly(L-γ-glutamylglutamine); PLGA, poly(D,L-lactide-co-glycolide); PTX, paclitaxel; SPION, superparamagnetic iron oxide NPs; *T*, therapeutic studies; TGN, blood–brain barrier-targeting peptide; TPGS, D-α-tocopheryl polyethylene glycol 1000 succinate. Cell lines: A375, human melanoma; A549, human lung cancer; B16-F10, murine melanoma; C26, murine colon cancer; C6, rat glioma; HeLa, human cervix cancer; HT29, human colorectal cancer; LNCaP, human prostate cancer; MDA-MB-231 and MCF-7, human breast cancer; OMM1.3 and Mel202, human melanoma; OVCAR3 and SKOV3, human ovarian cancer; U87 MG, human glioblastoma. Unless otherwise indicated, the percentages are in comparison to the control without the AS1411.

[a] Relative to NPs with control aptamer.

[b] Relative to nontargeted nanorobots.

[c] Relative to mice treated with saline, free thrombin, nontargeted nanorobots, or empty nanorobots.

TABLE 3

Nucleolin-binding pseudopeptides and derived agents

Name and format	*In vitro* effects	*In vivo* model	Schedule	*In vivo* effects	Refs
HB-19	↓ Colony formation (5 mM) MDA-MB-231, MDA-MB-435 PC-3, U87 MG, B16, and G401	Antiangiogenic effects: Swiss mice	1 mM HB-19	↓ Blood vessel density	[81,82,137]
	↓ Proliferation and migration of VEGF-stimulated HUVEC	Matrigel plug model Antitumoral effects: nude mice Right flank (MDA-MB-231) or mammary fat pad (MDA-MB-435)	i.p., sc., or peritumoral, 5 mg/kg, 3 times per week	↓ Tumor weight (95% and 57%, respectively)	
		MT/ret$^{+/-}$ transgenic mice (C57BL/6 background) Spontaneous melanoma model	i.p., 5 injections/week during weeks 1–3 and 2 injections/week during weeks 4–42; 50, 100, and 200 μg for the first, second, and rest of weeks, respectively	Delayed onset of cutaneous tumors and nodules	
		Nude mice 4×10^6 HB-19-treated G401 cells Ectopic (back)		↓ Tumorigenicity (50%)	
N6L	GI_{50} (72 h): 2.7–>40 mM Panel of 22 cell lines from different origins (lowest and highest values corresponding to HUVEC and Renca, respectively)	Nude mice Ectopic (right flank, MDA-MB-231 or PC3)	i.p. 1 g/kg 5 times/week	↓ Tumor volume (90% in MDA-MB-231, 40% in PC3)	[83,84,86]
	↓ HUVEC proliferation	Balb/c and C57BL/6 mice 5×10^6 A20 cells 5×10^5 T29 cells	i.p. 8 g/kg 5 times/week	↑ Survival (twofold in A20 and sixfold in T29)	
	↓ HUVEC adhesion (40%), proliferation and migration (61%) for 50 mM	Balb/c nude mice 1.5×10^5 U87-LUC cells Orthotopic	i.p.10 mg/kg, 5 days/week from day 1 post cell inoculation for 4 weeks	↑ Survival (50%)	
	↓ MIA PaCa2 and mPDAC migration (70%, for 50 mM)	FVB/n syngeneic mice 10^3 mPDAC cells Orthotopic	i.p. 10 mg/kg, 3 days/week, for 3 weeks	↓ Tumor volume (43.4%) ↓ Cell proliferation ↑ Apoptosis ↓ Liver metastasis area (67%) ↓ Vessel density (42%) ↓ Vessel branching (62%) ↑ Perfusion of tumor vasculature (>twofold) ↑ Pericyte coverage (70%) ↓ Hypoxic area (>50%)	
	↓ mPDAC invasion	RIP-Tag2 transgenic mice	i.p. 2 mg/kg N6L 3 days/week, for 1 week, followed by i.v. 100 mg/kg gemcitabine 2 days/week and i.p. 2 mg/kg N6L 3 days/week, for 2 weeks	↓ Tumor volume (75%)[a]	
	↑ HBVP migration		10 mg/kg, 3 days/week (from 12 to 16 weeks of age)	↓ Tumor growth (40%) ↑ Apoptosis (90%) ↓ Vessel density ↓ Vessel branching ↑ Perfusion of tumor vasculature	
N6L polyplexes	Similar effect on viability as N6L	NU/NU mice 5×10^6 PANC-1 cells Ectopic	i.p. 2 mg/kg N6L	↓ Tumor growth (85%) ↓ Cell proliferation (53%) ↓ Vasculature area (70%)	[87]
		FVB/n syngeneic mice 0.5×10^3 mPDAC cells	*BD*: i.v. N6L-Alexa Fluor488 polyplexes *T*: i.p. 10 mg/kg N6L, 3 times/week, for 3 weeks	↑ Accumulation in tumor compared with N6L ↓ Tumor volume by 45% (N6L) or 72% (N6L polyplexes)	

[109_TD$DIFF]TABLE 3 (*Continued*)

Name and format	*In vitro* effects	*In vivo* model	Schedule	*In vivo* effects	Refs
SAP-N6L (N6L cross-linked to saporin)	↓ Viability, IC_{50} (96 h), untargeted and targeted[b]: U87: 140 and 0.5 nM Primary glioblastoma cells: 13 and 0.0059 nM	Balb/c mice 1.5×10^5 U87-LUC cells Orthotopic	i.p. 0.5 mg/kg SAP-N6L, once/week, for 4 weeks	↓ Tumor growth	[88]

Cell lines: A20, murine lymphoma; B16, mouse melanoma; HBVP, human brain vascular pericytes; MDA-MB-231, human breast cancer; MIA PaCa2 and PANC-1, human pancreatic cancer; mPDAC, murine pancreatic cancer; MV4-11, human leukemia; PC-3, human prostate cancer; T29, human lymphoma; U87, human glioblastoma. Unless otherwise indicated, percentages indicated are in comparison to untreated cells/PBS-treated mice.
[a]Relative to single treatments.
[b]Without and with N6L, respectively.
[c]Relative to treatment with PBS or saporin.

TABLE 4

Anti-nucleolin antibodies

Name and format	*In vitro* effects	*In vivo* model	Administration	*In vivo* effects	Refs
NCL3 (rabbit IgG)	↓ HUVEC capillary-like tube formation (10 mg/ml) ↓ HUVEC viability (>50%), modest effect in C8161	Balb/c nude mice Matrigel plug model BALB/c nude mice 2×10^6 MDA-MB-435 cells Orthotopic	200 mg NCL3, daily, for 7 days i.v. 400 mg NCL3, every 3 days	↓ Blood vessel density No reduction in tumor growth ↓ Blood vessel density Normalization of tumor vasculature	[120]
Human IgGs	↓ MV4-11 viability (30–80%) CDC effect against MV4-11 cells	–	–	–	[121]
CP101.2C8 (human IgG)	↓ Viability of eight cell lines of different histological origins (IC_{50} at 96 h below 1 mg/ml)	MV14-11 human xenograft model	NA	30% of long-term survivors	[122]
4LB5 (human scFv)	↓ Viability IC_{50} (72 h): MDA-MB-231: 30 nM T47D: 20 nM BT549: 58 nM MDA-MB-436: 50 nM PLC-PRF: 3 nM	NOD-SCID mice 2×10^6 Luc^+MDA-MB-231 cells Orthotopic	i.p. 2 mg/kg, twice a week	↓ Tumor volume ↓ Cellularity ↓ Cell proliferation	[123]
4LB5-HP-RNase (human scFv fused to human pancreatic RNase)	↓ Viability IC_{50} (72 h): MDA-MB-231: 25 nM BT549: 12.5 nM MDA-MB-436: 50 nM MCF-7: 25 nM ↓ Colony formation of MDA-MB-231, BT549 and MDA-MB-436[c]	NOD-SCID mice 2×10^6 Luc^+MDA-MB-231 cells Orthotopic	i.p. 2 mg/kg, twice/week	↓ Tumor volume[a] ↓ Cellularity[a] ↑ Cell proliferation[a]	[124]
VHHs	↓ Viability, 8 mM MDA-MB-435S (80%) 4T1 (80%)	–	–	–	[125]
VHH-Fc	↓ Viability, 1 mM MDA-MB-435S (75%) 4T1 (75%) ADCC effect against MDA-MB-435S cells	–	–	–	[125]

Cell lines: 4T1, mouse breast cancer; BT549, MDA-MB-231, MDA-MB-436 and T47D, human breast cancer; C8161, human melanoma; HBVP, human brain vascular pericytes; MV4-11, human leukemia; PC-3, human prostate cancer; PLC-PRF, human hepatoma. Unless otherwise indicated, percentages indicated are in comparison to untreated cells/PBS-treated mice.
[a] Relative to treatment with 4LB5.

further demonstrated against rhabdoid tumor-derived cells, upon reducing the tumorigenic potential as well as the expression of different genes involved in tumorigenesis and angiogenesis, such as Wilms' tumor 1 (*WT1*), matrix metalloproteinase-2 (*MMP2*), the epithelial isoform of CD44 (*CD44E*) and *VEGF*. In TIII melanoma cells, it reduced the expression of *MMP2*, *MMP9*, and tumor necrosis factor alpha (*TNFa*) [82].

Among the different analogs generated from the original HB-19, the one codenamed N6L proved to be particularly promising [83]. N6L comprises six repeats of lysine-2-aminoisobutyric acid-gly-

cine, with the pseudotripeptide lysine-proline-arginine (reduced peptide bond between lysine and proline) grafted onto the lysine residues. In contrast to HB-19, characterized to translocated to the cytoplasm upon binding to nucleolin, N6L translocates to the nucleolus [83]. Interestingly, N6L enabled distinct inhibitory mechanisms in a tumor cell type-dependent manner, because 90% cell growth inhibition was observed for the most sensitive cell lines. In leukemia and lymphoma cell lines, it not only inhibited cell growth, but also promoted a level of cell death that varied between 35% and 70% [54]. Other N6L effects were also dependent on the tumor cell histological origin. In cell lines from breast, prostate, and cervical cancer, incubation with N6L restored contact inhibition, whereas inhibition of spreading and migration was observed in cell lines from colon carcinoma and breast cancer, respectively [54].

In agreement with the impact of N6L on cancer cell growth and death, studies exploring its effects at the molecular level reported alterations in apoptotic pathways and the cell cycle. In MDA-MB-231 breast cancer cells, N6L led to caspase-dependent apoptosis [83], whereas, in glioblastoma cells, it decreased the levels of cyclins D1 and B2, promoting an increased number of cells in G1 phase and cell cycle inhibition [84]. In addition, autophagy of glioblastoma cells, as evaluated by the expression of the autophagic markers p62, LC3I, and LC3II [84], was also observed.

Similar to other strategies targeting nucleolin, N6L also affected angiogenic endothelial cells. HUVEC cells incubated with N6L presented decreased adhesion, proliferation, and migration, consistent with the observed decreased expression of *MMP2* (involved in the degradation of the extracellular matrix and, therefore, in migration) and activation of several kinases [Src, focal adhesion kinase (FAK), Akt, and ERK1/2] that regulate cell adhesion and proliferation [85]. Also consistent with its antiproliferative effects, N6L increased the percentage of cells in G1 phase [86]. These effects translated into angiogenesis inhibition, evaluated by CAM assays [83].

Importantly, in endothelial cells, N6L also decreased the secretion or expression of angiopoietin 2 (Ang-2, after a 5-h or 72-h incubation, respectively), a protein that prevents vessel normalization, and increased expression of platelet-derived growth factor receptor beta (PDGFβ), involved in pericyte recruitment, which helps maintain the vasculature structure [86]. In fact, *in vitro* assays showed improved pericyte migration upon incubation with N6L. These results supported an effect of N6L on both cancer cells and tumor vasculature, which was further confirmed *in vivo*. In both xenograft and syngeneic models, N6L showed antitumoral and antiangiogenic properties with no associated toxicity [83,84,86]. In a syngeneic model of pancreatic cancer, treatment with N6L not only affected tumor volume and metastasis, but also promoted normalization of the tumor vasculature, by increasing pericyte coverage (which prevents vascularization) and reducing hypoxic area (evaluated by pimonidazole and carbonic anhydrase 9 staining) [86]. In line with the *in vitro* results, N6L-treated mice presented a 68% reduction in Ang-2 levels in the plasma, as well as decreased expression in the tumor. The tumor vasculature normalization resulted in improved perfusion and doxorubicin delivery, with a 3.5-fold increase in the tumor drug level. The positive impact of vasculature normalization was further confirmed in pancreatic tumors. N6L combined with gemcitabine, the standard of care in this setting, enabled significant tumor growth inhibition relative to single treatments [86]. Given these promising results, the potential of N6L was further assessed in a Phase I/IIa clinical trial on advanced solid tumors (NCT01711398), the results of which are not yet known.

Other N6L-based strategies have been developed, taking advantage of either its antitumoral effects (N6L polyplexes [87]) or its targeting ability (N6L-saporin construct [88] and iron oxide magnetic particles [89,90]). The development of N6L sulfated glycosaminoglycans polyplexes aimed to improve antitumoral effects through increased valency. This strategy proved successful, because N6L polyplexes decreased tumor growth, cell proliferation, and the vascular area in an ectopic model of pancreatic cancer, upon intraperitoneal (i.p.) injection, at concentrations at which N6L did not have an impact. In an orthotopic model of pancreatic cancer, administration of N6L led to decreased tumor volume, an effect that was more pronounced for N6L polyplexes. In fact, N6L polyplexes were more effective in reducing tumor volume than was gemcitabine, a standard of care for pancreatic cancer, without displaying systemic toxicity [87]. The increased N6L polyplexes accumulation in tumor relative to N6L alone suggested that the enhanced permeability and retention (EPR) effect explained the improved efficacy of the former. Therefore, this study confirmed the relevance of this kind of strategy, which could be further improved upon simultaneous delivery of a cytotoxic drug.

The use of N6L as a targeting ligand for NPs has been exploited in the context of iron oxide magnetic NPs, with the targeted NPs presenting increased accumulation in MDA-MB-231 breast tumors relative to the nontargeted counterparts [89]. Subsequent to this work, doxorubicin-loaded iron oxide targeted NPs for breast cancer thermotherapy presented improved MDA-MB-231 tumor growth inhibition relative to the nontargeted counterparts. However, the differences between targeted and untargeted NPs were dissipated upon the hyperthermic treatment [90]. Therefore, although N6L improved the therapeutic efficacy of doxorubicin delivery by NPs, a potential advantage of the combined hyperthermia and local chemotherapy was not observed.

Dhez *et al.* devised an alternative approach to take advantage of the N6L-targeting capacity by cross-linking it to saporin, a plant toxin of the ribosome-inactivating protein (RIP) family. This construct presented improved cytotoxicity against several cancer cell lines, including glioblastoma, as well as primary glioblastoma cells. In addition, it also enabled improved inhibition of neurosphere formation and of tumor growth in an *in vivo* glioblastoma orthotopic model [88].

Preclinical studies suggested that N6L is also promising for other diseases characterized by abnormal blood supply, such as diabetic retinopathy and macular degeneration (ImmuPharma PLC. Porfolio – Oncology and Ophtalmology; www.immupharma.co.uk/folio/oncologyopthamology/ [accessed 22 May 2019]).

Anti-nucleolin antibodies

Antibodies, also known as immunoglobulins (Ig), are proteins produced by B cells of the adaptive immune system in response to antigen detection. In mammals, antibodies are grouped into five isotypes (IgA, IgD, IgE, IgG, and IgM), each presenting a specific structure and role in immunological processes. The most common of these, IgG, accounts for up to 80% of the antibodies in normal serum and is usually one of the components of recombinant proteins for therapeutic purposes for several diseases, including many types of cancer [91]. Here, the antibody structure and

mechanisms of action, as well as recent advances in antibody engineering, are described and discussed within the frame of their impact on the development of novel strategies targeting nucleolin.

A typical antibody (Fig. 2) is a Y-shaped molecule that presents two main regions: the antigen-binding fragments (Fab) and the fragment crystallizable (Fc) region. Each Fab fragment presents two variable domains (variable heavy chain, VH, and variable light chain, VL), along with a constant region (CH1). Both VH and VL domains present three complementarity determining regions (CDR1, CDR2, and CDR3), which are responsible for the binding to the antigen. These domains also present four framework regions (FR) that act as scaffolds that support the loops of the CDRs. The remaining constant domains of the antibody, CH2 and CH3, constitute the fragment crystallizable (Fc). The Fc fragment is responsible for the prolonged serum half-life, typical of monoclonal antibodies, upon binding to the neonatal Fc receptor (FcRn), further transporting it within and across cells, thus preventing degradation.

The two Fabs are linked to the Fc region by the hinge region, a flexible linker that impacts the flexibility of the molecule [92]. Differences in the amino acid composition and structure of the hinge region are the main characteristics for grouping IgGs in four subclasses (from IgG1 to IgG4). IgG1 and IgG3 are more prone to trigger immune functions, the former presenting the strongest antibody-dependent cellular cytotoxicity (ADCC) activity, and the latter the strongest Complement-dependent cytotoxicity (CDC) capacity [92].

In terms of serum stability, IgG3 is the least stable, with a serum half-life of 7 days. The other subclasses present half-lives of 21 days, which make them more adequate for therapeutic applications. Therefore, IgG2 or IgG4 are the preferential choices when immune responses arising from the release of proinflammatory cytokines are undesirable, as in inflammatory and autoimmune disorders. For diseases in which immune functions have a beneficial effect, such as cancer and viral diseases, IgG1 is the subclass of preference [92].

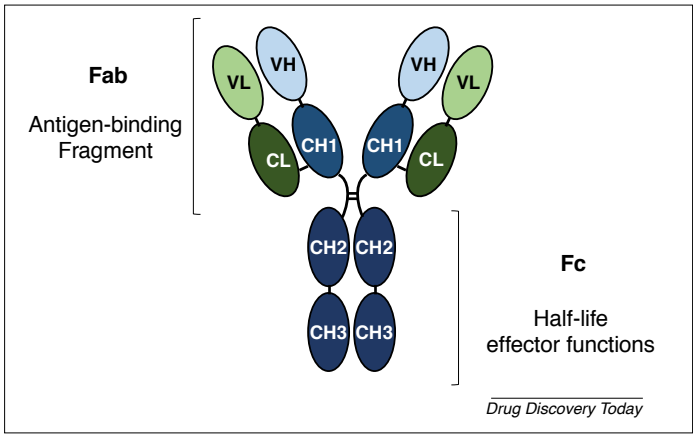

FIGURE 2

Structure of a canonical immunoglobulin (Ig)-G1 antibody. IgGs are homodimeric proteins, with both constant (C) and variable (V) domains that organize into light (L) and heavy (H) chains. IgGs present two main regions: the antigen-binding fragments (Fab), which bind to the antibody target with high affinity and specificity, and the fragment crystallizable (Fc) region, responsible for triggering immune responses upon binding to the matching receptor in cells of the immune system. The specificity of the antibody towards different targets derives from highly variable sequences of loops in the Fabs, the complementary-determining regions (CDRs), which are present both in the light and the heavy chains.

Antibodies can exert their effects by several mechanisms, ranging from inducing direct cell death to the recruitment of components of the immune system. Antibody binding to its target, such as trastuzumab, bevacizumab, or cetuximab, can alter signal transduction pathways that are involved in cell proliferation and survival, thus switching off the overall proliferative capacity of these cells. Conversely, antibodies can act as receptor agonists and can be used to trigger signaling cascades that lead to cell cycle arrest and apoptosis., as is the case of apomab, which binds the death receptor 5 (DR5). In addition to these target-specific effects, antibodies can act by recruiting effectors of the immune system, either cells or complement factors, leading to ADCC or CDC mechanisms, respectively [93–96].

ADCC is triggered by the simultaneous binding of an antibody to its target cell, through the Fab domains, and to cells of the immune system [mainly natural killer (NK) cells], through the Fc region. This double binding initiates a signaling pathway in the effector cells of the immune system that culminates in the release of several toxins into target cells the antibody is bound to, thus leading to cell death [97].

The importance of ADCC in the therapeutic outcome of patients' has been validated in several studies involving polymorphisms in the IgG1 Fc receptor-encoding *FcγRIIA* and *FcγRIIIA* genes. FcγRIIa and FcγRIIIa/CD16a are low-affinity activating receptors for IgG1 Fc and are expressed by subpopulations of NK cells, macrophages, or T cells. Some polymorphisms in these genes augment the affinity of the IgG1 Fc region towards the receptor, which correlated with better clinical responses, relative to cohorts without polymorphisms. This type of association has been observed in patients treated with cetuximab [98], trastuzumab [99,100], or rituximab [101,102]. Some of these studies also comprised an *ex-vivo* ADCC assay using peripheral blood mononuclear cells (PBMCs) or NK cells from both cohorts of patients (with and without polymorphisms). The ADCC capacity of immune cells was increased in the cohort of patients presenting the aforementioned polymorphisms, consistent with a better clinical response, and further supporting the importance of this cell death mechanism [99,103–106]. Interestingly, one of these studies, assessing trastuzumab activity in patients with HER2+ metastatic breast cancer even suggested ADCC as the main mechanism of action of trastuzumab in this setting. This was supported by the fact that the association between better clinical response and Fc receptor polymorphisms was observed in the context of the absence of HER2 downmodulation and of changes in cell proliferation [105]. Taken together, these studies support the ADCC mechanism as a relevant component in the therapeutic efficacy of antibodies, at least in some therapeutic settings.

Similar to the ADCC mechanism, CDC responses are also triggered by a simultaneous binding of the antibody to the target cell and to effector components. However, in this case, C1q replaces immune cells as the effector component and its binding to antigen–antibody complexes initiates the classic complement pathway. This pathway culminates in the assembly of the membrane attack complex (MAC), which leads to the formation of pores in the cell membrane and consequent death. This process also results in the recruitment of phagocytes, further promoting cell death [107]. Although the relevance of CDC for the antibody therapeutic efficacy remains largely unexplored, *in vivo* studies in a

CD20-overexpressing EL4 lymphoma model suggested the importance of this mechanism in the activity of rituximab. In fact, although rituximab led to improved survival in this model, this effect was absent in a similar model that lacked C1q. Conversely, depletion of NK cells and/or neutrophils did not affect the therapeutic efficacy of the antibody [108]. Similar results were observed in a CD20-overexpressing 38C13 lymphoma model [109].

Although antibodies are an important component in the treatment of several types of cancer and other diseases, they present some characteristics that limit their therapeutic efficacy. In the case of the treatment of solid tumors, the main disadvantage arises from their high molecular weight (150 kDa), which limits tumor penetration [110]. As a result, a plethora of antibody fragments has been generated (Fig. 3).

Research on antibody fragment initially focused on the use of single Fabs, because they can be obtained from the monoclonal antibody by proteolytic cleavage with papain. This enables a ~50-kDa antibody format, subsequent to the absence of the Fc region. The development of recombinant technologies provided a way to further explore different formats, such as a single-chain fragment variable (scFv), in which the VH and VL domains are joined by a linker that confers stability to the resulting protein. Production of smaller functional fragments (VH or VL) proved ineffective, because these fragments do not fold properly, are water insoluble and aggregate because of the exposure of hydrophobic amino acids within the VH–VL interface. Therefore, scFv was the smallest functional fragment that could be successfully used [111,112].

However, in 1993, Hamers-Casterman *et al.* identified camel antibodies in which the light chains and CH1 domain were absent [113], resulting in an antigen-binding region comprising a single VH in each arm. These smaller antibodies (100 kDa) endowed an extensive antigen-binding repertoire and retained high affinity to the antigen [114]. The discovery of these naturally occurring noncanonical antibodies, named heavy chain antibodies (HCAbs), showed that different antibody formats could be obtained in a stable and effective form. This further paved the way to the development of a new class of antibody fragments, including camelid VHs, named variable region of a heavy chain antibodies (VHHs). In addition to their small size, VHHs display long surface loops that enable them to reach target antigens that are not usually recognized. In HCabs, the CDR3 is usually longer than the human VH CDR3, which might account for the VHH effectiveness in target binding, even in the absence of the VL [115,116].

One of the main advantages of these smaller antibody formats (Fab, scFv, and VHH) arises from their versatility to originate diverse protein formats. They can be engineered to originate bifunctional molecules (upon linking or genetically fusing them to a molecule with the desired function), multimerized, or altered to present bispecificity or even trispecificity, and their blood half-life can be adapted according to the application [117]. This has been exemplified by the variety of targeting strategies, based on antibody fragments, developed against EGFR.

Other strategies that have been explored in the context of other cancer targets include VHH fusion to a Fc region, a format that not only enables improved accumulation in tumors, relative to VHHs in monomeric or pentameric format [118], but also has the potential to trigger immune responses [119].

Antibody-based constructs against nucleolin have also been explored, such as NCL3, a rabbit nucleolin-binding full-length antibody, the effects of which were mainly seen at the tumor vasculature level. NCL3 decreased viability of both angiogenic endothelial (HUVEC) and melanoma (C8161) cells, but this effect was more pronounced in the former and was accompanied by downregulation of Bcl-2 expression. *In vivo*, this translated into

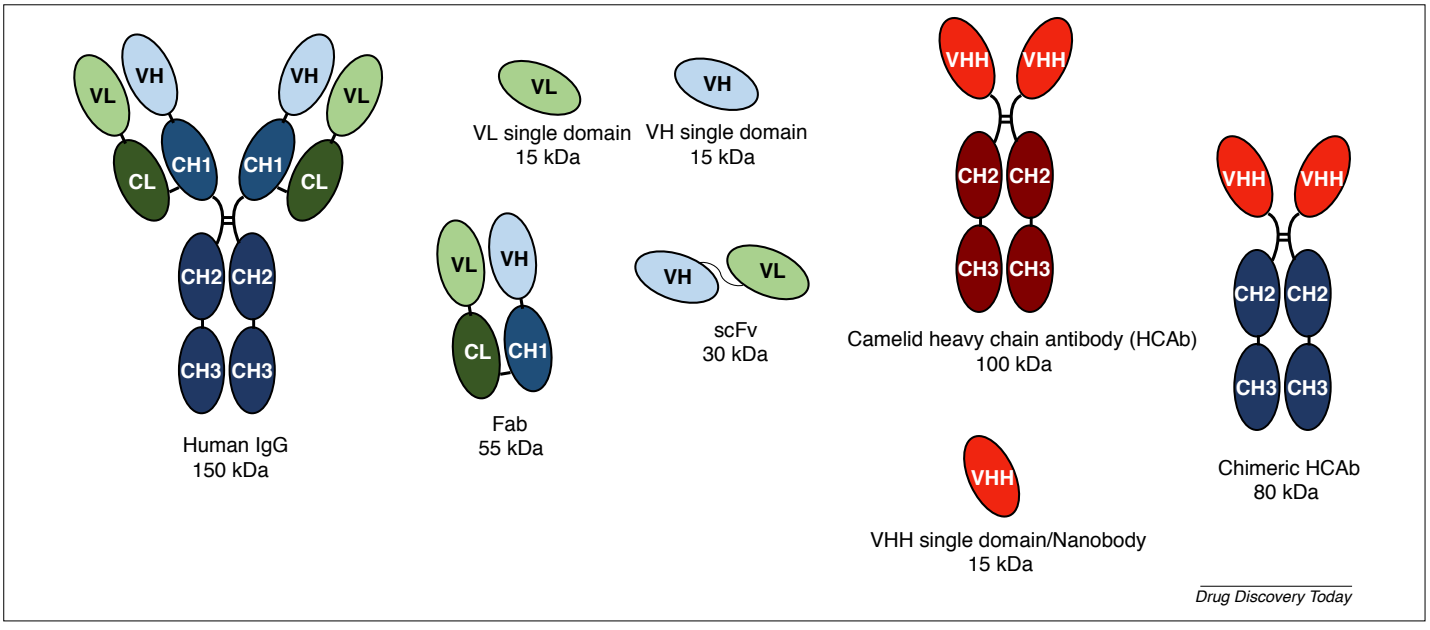

FIGURE 3

Schematic representation of antibody formats. Both canonical [immunoglobulin (Ig)G] and non-canonical (camelid) immunoglobulins are depicted, as well as examples of other antibody formats that can be generated. These formats include not only fragments obtained from the full IgG, such as single domains and Fabs, but also those originated upon combining different fragments. For each format, their approximate size in kilodaltons is indicated.

decreased density of blood vessels in a Matrigel plug model relative to mice treated with saline or control rabbit IgG. The same effect was observed in the MDA-MB-435 murine model, whereas tumor volume did not vary among the three groups. However, evaluation of tumor vasculature structure upon NCL3 administration suggested that this antibody promoted vasculature normalization. This was supported by the fact that tumors from NCL3-treated mice presented more homogeneous and less tortuous vasculature compared with control-treated mice. In addition, the former presented increased pericyte coverage and basement membrane deposition in the vasculature (evaluated by immunostaining with CD31 and NG2 or collagen IV, respectively), further supporting vasculature normalization. Consistent with these results, NCL3 administration resulted in decreased tumor hypoxia [120].

The generation of antinucleolin full-length human antibodies has also been reported. These antibodies reduced the viability of leukemic MV4-11 cells, from 30–80% compared with untreated cells. Given the differences between human and rabbit Fc regions (which characterizes NCL3), the latter does not trigger immune responses, such as ADCC and CDC, upon incubation with human effector components (human PBMCs or complement). In fact, some of these full-length human antibodies presented increased cytotoxic activity in the presence of human serum (a source of complement), relative to the control condition using heat-inactivated human serum, thus suggesting a CDC effect [121]. One of these antibodies, CP101.2C8, which binds to RBDs of nucleolin, has proven particularly promising against a MV4-11 xenograft mouse model of leukemia, resulting in 30% of mice surviving long-term, relative to an IgG isotype control [122].

The plethora of alternative antibody formats that can be generated, allowing a variety of effects, has also been explored in the context of nucleolin targeting. Two main formats have been developed, scFv and VHH, which have be further explored following different strategies.

The antinucleolin RBD-binding scFv 4LB5, isolated by phage display from the CDR3-randomized Griffin.1 library, affected the viability and proliferation of different breast cancer lines, as well as a hepatoma cell line. In addition, impaired cell migration was observed for two of the breast cancer cell lines upon incubation with 4LB5. Activity was supported by the downregulation of miR-21, miR-221, and miR-222, and increased apoptosis, evaluated by cell staining with propidium iodide and western blot analysis of poly(ADP-ribose) polymerase. Consistently, 4LB5 treatment reduced AKT levels and activated caspase 3/7. 4LB5 administration in an *in vivo* breast cancer model led to decreased tumor growth, without evidence of adverse effects. Tumors from treated mice presented reduced cellularity, as well as necrotic areas [123]. Fusion of 4LB5 to human pancreatic RNase, which becomes toxic upon internalization, resulted in a significant reduction in colony formation and tumor growth inhibition, relative to 4LB5 alone. Similar to 4LB5 alone, the fusion construct enabled apoptosis and reduced the levels of miR-21, miR-221, and miR-222. The reduction in miRNA levels was more pronounced for 4LB5-HP-RNase than for 4LB5, suggesting a contribution of the RNase moiety. Although tumors from mice treated with this fusion construct presented reduced cellularity compared with those treated with 4LB5, proliferation increased. These results suggested that this construct acted mainly through a cytotoxic rather than a cytostatic effect [124].

Several antinucleolin VHHs have also been developed, using a grafting strategy based on the F3 peptide. A 10-amino acid nucleolin-binding sequence of this peptide was grafted onto CDR1 or CDR3 of a parental VHH, because these CDRs usually present the highest binding extent to the antigen [115,116]. The novel VHHs presented binding to cancer cell lines as well as cytotoxic activity against the same cells, in the micromolar range. Variants of these VHHs, in which the 10-amino acid sequence was flanked by the SGGGS linker to confer increased flexibility to the CDR, did not change the binding or cytotoxicity activity. The CDR3-grafted VHH was further fused to the Fc region of a human IgG1, which resulted in cytotoxicity in the nanomolar range and enabled an ADCC effect against MDA-MB-435S cancer cells [125].

Concluding remarks

Given its overexpression at the cell surface in several tumor compartments, including the more accessible tumor vasculature, nucleolin is a promising target for anticancer therapy. Collectively, the studies herein presented and discussed, illustrate the potential of antibody-based approaches for nucleolin targeting, allowing the generation of entities with different mechanisms of action. Importantly, similar to what has been performed with F3 peptide and AS1411, all the antibody formats described herein could also be used for targeted delivery with NPs, further expanding their versatility. Thus, antibody engineering offers a variety of novel strategies for nucleolin-based targeting in cancer treatment. Of relevance, antibody-based strategies have opened the field of antinucleolin immunotherapeutic approaches, thus expanding the potential of nucleolin-targeting strategies.

Acknowledgments

S.R. was a student of the PhD Program in Experimental Biology and Biomedicine (PDBEB), Center for Neuroscience and Cell Biology, University of Coimbra, and recipient of the fellowship SFRH/BD/51680/2011 from the Portuguese Foundation for Science and Technology. This work was also financed by the European Regional Development Fund (ERDF), through the Centro 2020 Regional Operational Programme under project CENTRO-01-0145-FEDER-000012 (HealthyAging2020), and through the COMPETE 2020 Operational Programme for Competitiveness and Internationalisation and Portuguese national funds via FCT – Fundação para a Ciência e a Tecnologia, I.P., under projects POCI-01-0145-FEDER-016390 (Cancel Stem), Euronanomed (FCT reference ENMed/0005/2015) and CNC.IBILI (FCT reference UID/NEU/04539/2019).

References

1 Bray, F. *et al.* (2018) Global Cancer Statistics 2018: GLOBOCAN estimates of incidence and mortality worldwide for 36 cancers in 185 countries. *CA Cancer J. Clin.* 68, 394–424

2 Nounou, M.I. *et al.* (2015) Breast cancer: conventional diagnosis and treatment modalities and recent patents and technologies. *Breast Cancer Basic Clin. Res.* 9, 17–34

3 Schmadeka, R. *et al.* (2014) Triple-negative breast carcinoma: current and emerging concepts. *Am. J. Clin. Pathol.* 141, 462–477
4 Tomao, F. *et al.* (2015) Triple-negative breast cancer: New perspectives for targeted therapies. *Oncol. Targets Ther.* 8, 177–193
5 Hanahan, D. and Weinberg, R.A. (2011) Hallmarks of cancer: the next generation. *Cell* 144, 646–674
6 Hanahan, D. and Coussens, L.M. (2012) Accessories to the crime: functions of cells recruited to the tumor microenvironment. *Cancer Cell* 21, 309–322
7 Yuan, Y. *et al.* (2016) Role of the tumor microenvironment in tumor progression and the clinical applications. *Oncol. Rep.* 35, 2499–2515
8 Fukumura, D. and Jain, R.K. (2008) Tumor microvasculature and microenvironment- Targets for antiangiogenesis and normalization. *Microvasc. Res.* 141, 520–529
9 Harlozinska, A. (2005) Progress in molecular mechanisms of tumor metastasis and angiogenesis. *Anticancer Res.* 3334, 3327–3333
10 Ebos, J.M.L. and Kerbe, R.S. (2011) Antiangiogenic therapy: impact on invasion, disease progression, and metastasis. *Nat. Rev. Clin. Oncol.* 8, 210–221
11 Ariffin, A.B. *et al.* (2014) Releasing pressure in tumors: What do we know so far and where do we go from here a review. *Cancer Res.* 74, 2655–2662
12 Liu, T. *et al.* (2011) Combination gene therapy using VEGF-shRNA and fusion suicide gene yCDglyTK inhibits gastric carcinoma growth. *Exp. Mol. Pathol.* 91, 745–752
13 Huang, S. *et al.* (2013) Tumor-targeting and smart nanoparticles for combination therapy of angiogenesis and apoptosis. *ACS Nano.* 7, 2860–2871
14 Orrick, L.R. *et al.* (1973) Comparison of nucleolar proteins of normal rat liver and Novikoff hepatoma ascites cells by two-dimensional polyacrylamide gel electrophoresis. *Proc. Natl. Acad. Sci. U. S. A.* 70, 1316–1320
15 Bugler, B. *et al.* (1982) Detection and localization of a class of proteins immunologically related to a 100-kDa nucleolar protein. *Eur. J. Biochem.* 128, 475–480
16 Roussel, P. and Hernandez-Verdun, D. (1994) Identification of Ag-NOR proteins, markers of proliferation related to ribosomal gene activity. *Exp. Cell Res.* 214, 465–472
17 Ginisty, H. *et al.* (1999) Structure and functions of nucleolin. *J. Cell Sci.* 112, 761–772
18 Srivastava, M. and Pollard, H.B. (1999) Molecular dissection of nucleolin's role in growth and cell proliferation: new insights. *FASEB J.* 13, 1911–1922
19 Tajrishi, M.M. *et al.* (2011) Nucleolin: The most abundant multifunctional phosphoprotein of nucleolus. *Commun. Integr. Biol.* 4, 267–275
20 Hovanessian, A.G. *et al.* (2000) The cell-surface-expressed nucleolin is associated with the actin cytoskeleton. *Exp. Cell Res.* 261, 312–328
21 Christian, S. *et al.* (2003) Nucleolin expressed at the cell surface is a marker of endothelial cells in angiogenic blood vessels. *J. Cell Biol.* 163, 871–878
22 Ding, Y. *et al.* (2012) Heat shock cognate 70 regulates the translocation and angiogenic function of nucleolin. *Arter. Thromb. Vasc. Biol.* 32, e126–e134
23 Huang, Y. *et al.* (2006) The angiogenic function of nucleolin is mediated by vascular endothelial growth factor and nonmuscle myosin. *Blood* 107, 3564–3571
24 Schwab, M. and Dreyer, C. (1997) Protein phosphorylation sites regulate the function of the bipartite NLS of nucleolin. *Eur. J. Cell Biol.* 73, 287–297
25 Fonseca, N.A. *et al.* (2015) Nucleolin overexpression in breast cancer cell sub-populations with different stem-like phenotype enables targeted intracellular delivery of synergistic drug combination. *Biomaterials* 69, 76–88
26 Visvader, J.E. and Lindeman, G.J. (2012) Cancer stem cells: current status and evolving complexities. *Cell Stem Cell* 10, 717–728
27 Pattabiraman, D.R. and Weinberg, R.A. (2014) Tackling the cancer stem cells - what challenges do they pose? *Nat. Rev. Drug Discov.* 13, 497–512
28 Fonseca, N.A. *et al.* (2017) The cancer stem cell phenotype as a determinant factor of the heterotypic nature of breast tumors. *Crit. Rev. Oncol. Hematol.* 113, 111–121
29 Zhuo, W. *et al.* (2010) Endostatin inhibits tumour lymphangiogenesis and lymphatic metastasis via cell surface nucleolin on lymphangiogenic endothelial cells. *J. Pathol.* 222, 249–260
30 Shi, H. *et al.* (2007) Nucleolin is a receptor that mediates antiangiogenic and antitumor activity of endostatin. *Blood* 110, 2899–2906
31 Porkka, K. *et al.* (2002) A fragment of the HMGN2 protein homes to the nuclei of tumor cells and tumor endothelial cells *in vivo*. *Proc. Natl. Acad. Sci. U. S. A.* 99, 7444–7449
32 Mahotka, C. *et al.* (2018) Nucleolin promotes execution of the hematopoietic stem cell gene expression program. *Leukemia* 32, 1865–1868
33 Zhang, J. *et al.* (2015) Nucleolin targeting AS1411 aptamer modified pH-sensitive micelles for enhanced delivery and antitumor efficacy of paclitaxel. *Nano Res.* 8, 201–218
34 Li, F. *et al.* (2017) A water-soluble nucleolin aptamer-paclitaxel conjugate for tumor-specific targeting in ovarian cancer. *Nat. Commun.* 8, 1390
35 Gregório, A.C. *et al.* (2018) Meeting the needs of breast cancer: a nucleolin's perspective. *Crit. Rev. Oncol. Hematol.* 125, 89–101
36 Hovanessian, A.G. *et al.* (2010) Surface expressed nucleolin is constantly induced in tumor cells to mediate calcium-dependent ligand internalization. *PLoS ONE* 5, e15787
37 Stepanova, V. *et al.* (2008) Nuclear translocation of urokinase-type plasminogen activator. *Blood* 112, 100–110
38 Said, E.A. *et al.* (2002) The anti-HIV cytokine midkine binds the cell surface-expressed nucleolin as a low affinity receptor. *J. Biol. Chem.* 277, 37492–37502
39 Said, E.A. *et al.* (2005) Pleiotrophin inhibits HIV infection by binding the cell surface-expressed nucleolin. *FEBS J.* 272, 4646–4659
40 Legrand, D. *et al.* (2004) Surface nucleolin participates in both the binding and endocytosis of lactoferrin in target cells. *Eur. J. Biochem.* 271, 303–317
41 Di Segni, A. *et al.* (2008) Identification of nucleolin as new ErbB receptors-interacting protein. *PLoS ONE* 3, e2310
42 Farin, K. *et al.* (2011) Oncogenic synergism between ErbB1, nucleolin, and mutant Ras. *Cancer Res.* 71, 2140–2151
43 Schokoroy, S. *et al.* (2013) Disrupting the oncogenic synergism between nucleolin and Ras results in cell growth inhibition and cell death. *PLoS ONE* 8, e75269
44 Goldshmit, Y. *et al.* (2014) Interfering with the interaction between ErbB1, nucleolin and Ras as a potential treatment for glioblastoma. *Oncotarget* 5, 8602–8613
45 Wolfson, E. *et al.* (2016) Nucleolin-binding by ErbB2 enhances tumorigenicity of ErbB2-positive breast cancer. *Oncotarget* 7, 65320–65334
46 Wolfson, E. *et al.* (2018) Nucleolin and ErbB2 inhibition reduces tumorigenicity of ErbB2-positive breast cancer. *Cell Death Dis.* 9, 47
47 Wise, J.F. *et al.* (2013) Nucleolin inhibits Fas ligand binding and suppresses Fas-mediated apoptosis *in vivo* via a surface nucleolin-Fas complex. *Blood* 121, 4729–4739
48 Tate, A. *et al.* (2006) Met-independent hepatocyte growth factor-mediated regulation of cell adhesion in human prostate cancer cells. *BMC Cancer* 6, 197
49 Chen, S.-C. *et al.* (2015) Hepatoma-derived growth factor/nucleolin axis as a novel oncogenic pathway in liver carcinogenesis. *Oncotarget* 6, 16253–16270
50 Yang, X. *et al.* (2014) Cell surface nucleolin is crucial in the activation of the CXCL12/CXCR4 signaling pathway. *Tumor Biol.* 35, 333–338
51 Lv, S. *et al.* (2014) Cell surface protein C23 affects EGF-EGFR induced activation of ERK and PI3K-AKT pathways. *J. Mol. Neurosci.* 55, 519–524
52 Dai, C. *et al.* (2014) Nuclear protein C23 on the cell surface plays an important role in activation of CXCR4 signaling in glioblastoma. *Mol. Neurobiol.* 52, 1521–1526
53 Koutsioumpa, M. *et al.* (2013) Interplay between avb3 integrin and nucleolin regulates human endothelial and glioma cell migration. *J. Biol. Chem.* 288, 343–354
54 Krust, B. *et al.* (2011) Targeting surface nucleolin with multivalent HB-19 and related Nucant pseudopeptides results in distinct inhibitory mechanisms depending on the malignant tumor cell type. *BMC Cancer* 11, 333
55 Moura, V. *et al.* (2012) Targeted and intracellular triggered delivery of therapeutics to cancer cells and the tumor microenvironment: impact on the treatment of breast cancer. *Breast Cancer Res. Treat.* 133, 61–73
56 Winer, I. *et al.* (2010) F3-targeted cisplatin-hydrogel nanoparticles as an effective therapeutic that targets both murine and human ovarian tumor endothelial cells *in vivo*. *Cancer Res.* 70, 8674–8683
57 Reddy, G.R. *et al.* (2006) Vascular targeted nanoparticles for imaging and treatment of brain tumors. *Clin. Cancer Res.* 12, 6677–6686
58 Drecoll, E. *et al.* (2009) Treatment of peritoneal carcinomatosis by targeted delivery of the radio-labeled tumor homing peptide Bi-DTPA-F32 into the nucleus of tumor cells. *PLoS ONE* 4, e5715
59 Fonseca, N.A. *et al.* (2014) Simultaneous active intracellular delivery of doxorubicin and C6-ceramide shifts the additive/antagonistic drug interaction of non-encapsulated combination. *J. Control. Release* 196, 122–131
60 Gomes-da-Silva, L.C. *et al.* (2014) Challenging the future of siRNA therapeutics against cancer: the crucial role of nanotechnology. *Cell Mol. Life Sci.* 71, 1417–1438
61 Gomes-da-Silva, L. *et al.* (2013) Efficient intracellular delivery of siRNA with a safe multitargeted lipid-based nanoplatform. *Nanomedicine* 8, 1397–1413
62 Gomes-Da-Silva, L.C. *et al.* (2013) Impact of anti-PLK1 siRNA-containing F3-targeted liposomes on the viability of both cancer and endothelial cells. *Eur. J. Pharm. Biopharm.* 85, 356–364
63 Shin, M.C. *et al.* (2017) Tandem-multimeric F3-gelonin fusion toxins for enhanced anti-cancer activity for prostate cancer treatment. *Int. J. Pharm.* 524, 101–110
64 Arumugam, S. *et al.* (2010) Solution structure of the RBD1,2 domains from human nucleolin. *J. Biomol. NMR* 47, 79–83
65 Li, L. *et al.* (2014) Nucleolin-targeting liposomes guided by aptamer AS1411 for the delivery of siRNA for the treatment of malignant melanomas. *Biomaterials* 35, 3840–3850

66 Guo, J. *et al.* (2011) Aptamer-functionalized PEG-PLGA nanoparticles for enhanced anti-glioma drug delivery. *Biomaterials* 32, 8010–8020
67 Li, Z. *et al.* (2012) Aptamer-capped multifunctional mesoporous strontium hydroxyapatite nanovehicle for cancer-cell-responsive drug delivery and imaging. *Biomacromolecules* 13, 4257–4263
68 Song, C. *et al.* (2013) Nucleolin targeting AS1411 modified protein nanoparticle for antitumor drugs delivery. *Mol. Pharm.* 10, 3555–3563
69 Latorre, A. *et al.* (2014) DNA and aptamer stabilized gold nanoparticles for targeted delivery of anticancer therapeutics. *Nanoscale* 6, 7436–7442
70 Ai, J. *et al.* (2014) Multifunctional AS1411-functionalized fluorescent gold nanoparticles for targeted cancer cell imaging and efficient photodynamic therapy. *Talanta* 118, 54–60
71 Gao, H. *et al.* (2012) Precise glioma targeting of and penetration by aptamer and peptide dual-functioned nanoparticles. *Biomaterials* 33, 5115–5123
72 Li, X. *et al.* (2016) Constructing aptamer anchored nanovesicles for enhanced tumor penetration and cellular uptake of water soluble chemotherapeutics. *Acta Biomater.* 35, 269–279
73 Luo, Z. *et al.* (2017) Precise glioblastoma targeting by AS1411 aptamer-functionalized poly (l-γ-glutamylglutamine)–paclitaxel nanoconjugates. *J. Colloid. Interface Sci* 490, 783–796
74 Li, S. *et al.* (2018) A DNA nanorobot functions as a cancer therapeutic in response to a molecular trigger *in vivo*. *Nat. Biotechnol.* 258–264
75 Soundararajan, S. *et al.* (2008) The nucleolin targeting aptamer AS1411 destabilizes Bcl-2 messenger RNA in human breast cancer cells. *Cancer Res.* 68, 2358–2365
76 Pichiorri, F. *et al.* (2013) *In vivo* NCL targeting affects breast cancer aggressiveness through miRNA regulation. *J. Exp. Med.* 210, 951–968
77 Girvan, A.C. *et al.* (2006) AGRO100 inhibits activation of nuclear factor-kB (NF-kB) by forming a complex with NF-kB essential modulator (NEMO) and nucleolin. *Mol. Cancer Ther.* 5, 1790–1799
78 Bates, P.J. *et al.* (2009) Discovery and development of the G-rich oligonucleotide AS1411 as a novel treatment for cancer. *Exp. Mol. Pathol.* 86, 151–164
79 Callebaut, C. *et al.* (1996) Inhibition of HIV infection by pseudopeptides blocking viral envelope glycoprotein-mediated membrane fusion and cell death. *Virology* 218, 181–192
80 Nisole, S. *et al.* (2002) The anti-HIV pentameric pseudopeptide HB-19 binds the C-terminal end of nucleolin and prevents anchorage of virus particles in the plasma membrane of target Cells. *J. Biol. Chem.* 277, 20877–20886
81 Destouches, D. *et al.* (2008) Suppression of tumor growth and angiogenesis by a specific antagonist of the cell-surface expressed nucleolin. *PLoS ONE* 3, e2518
82 El Khoury, D. *et al.* (2010) Targeting surface nucleolin with a multivalent pseudopeptide delays development of spontaneous melanoma in RET transgenic mice. *BMC Cancer* 10, 325
83 Destouches, D. *et al.* (2011) A simple approach to cancer therapy afforded by multivalent pseudopeptides that target cell-surface nucleoproteins. *Cancer Res.* 71, 3296–3305
84 Benedetti, E. *et al.* (2015) Nucleolin antagonist triggers autophagic cell death in human glioblastoma primary cells and decreased *in vivo* tumor growth in orthotopic brain tumor model. *Oncotarget* 6, 42091–42104
85 Birmpas, C. *et al.* (2012) Nucleolin mediates the antiangiogenesis effect of the pseudopeptide N6L. *BMC Cell Biol.* 13, 32
86 Gilles, M.-E. *et al.* (2016) Nucleolin targeting impairs the progression of pancreatic cancer and promotes the normalization of tumor vasculature. *Cancer Res.* 7181–7193
87 Diamantopoulou, Z. *et al.* (2017) Multivalent cationic pseudopeptide polyplexes as a tool for cancer therapy. *Oncotarget* 8, 90108–90122
88 Anne-Chloé, D. *et al.* (2017) Targeted therapy of human glioblastoma via delivery of a toxin through a peptide directed to cell surface nucleolin. *J. Cell Physiol.* 4091–4105
89 Pierre Couleaud, M.S. (2015) Functionalization of iron oxide magnetic nanoparticles with the multivalent pseudopeptide N6l for breast tumor targeting. *J. Nanomed. Nanotechnol.* 06, 4–11
90 Kossatz, S. *et al.* (2015) Efficient treatment of breast cancer xenografts with multifunctionalized iron oxide nanoparticles combining magnetic hyperthermia and anti-cancer drug delivery. *Breast Cancer Res.* 17, 66
91 Adams, G.P. and Weiner, L.M. (2005) Monoclonal antibody therapy of cancer. *Nat. Biotechnol* 23, 1147–1157
92 Vidarsson, G. *et al.* (2014) IgG subclasses and allotypes: from structure to effector functions. *Front. Immunol.* 5, 1–17
93 Weiner, L.M. *et al.* (2010) Monoclonal antibodies: versatile platforms for cancer immunotherapy. *Nat. Rev. Immunol* 10, 317–327
94 Golay, J. and Introna, M. (2012) Mechanism of action of therapeutic monoclonal antibodies: Promises and pitfalls of *in vitro* and *in vivo* assays. *Arch. Biochem. Biophys.* 526, 146–153
95 Redman, J.M. *et al.* (2015) Mechanisms of action of therapeutic antibodies for cancer. *Mol. Immunol.* 67, 28–45
96 Carter, P. (2001) Improving the efficacy of antibody-based cancer therapies. *Nat. Rev. Cancer* 1, 118–129
97 Lieberman, J. (2003) The ABCs of granule-mediated cytotoxicity: new weapons in the arsenal. *Nat. Rev. Immunol* 3, 361–370
98 Bibeau, F. *et al.* (2009) Impact of Fc RIIa-Fc RIIIa polymorphisms and KRAS mutations on the clinical outcome of patients with metastatic colorectal cancer treated with cetuximab plus irinotecan. *J. Clin. Oncol.* 27, 1122–1129
99 Musolino, A. *et al.* (2008) Immunoglobulin G fragment c receptor polymorphisms and clinical efficacy of trastuzumab-based therapy in patients with HER-2/neu-positive metastatic breast cancer. *J. Clin. Oncol.* 26, 1789–1796
100 Wang, D.-S. *et al.* (2017) FcγRIIA and IIIA polymorphisms predict clinical outcome of trastuzumab-treated metastatic gastric cancer. *Oncol. Targets Ther.* 10, 5065–5076
101 Cartron, G. *et al.* (2002) Therapeutic activity of humanized anti-CD20 monoclonal antibody and polymorphism in IgG Fc receptor FcγrIIIa gene. *Blood* 99, 754–758
102 Paiva, M. *et al.* (2008) FcγRIIa polymorphism and clinical response to rituximab in non-Hodgkin lymphoma patients. *Cancer Genet. Cytogenet.* 183, 35–40
103 López-Albaitero, A. *et al.* (2009) Role of polymorphic Fc gamma receptor IIIa and EGFR expression level in cetuximab mediated, NK cell dependent *in vitro* cytotoxicity of head and neck squamous cell carcinoma cells. *Cancer Immunol. Immunother.* 58, 1853–1864
104 Taylor, R.J. *et al.* (2009) FcgRIIIa polymorphisms and cetuximab induced cytotoxicity in squamous cell carcinoma of the head and neck. *Cancer Immunol. Immunother.* 58, 997–1006
105 Gennari, R. *et al.* (2004) Pilot study of the mechanism of action of preoperative trastuzumab in patients with primary operable breast tumors overexpressing HER2. *Clin. Cancer Res.* 10, 5650–5655
106 Ozzo, S.D. *et al.* (2004) Rituximab-dependent cytotoxicity by natural killer cells: influence of FCGR3A polymorphism on the concentration-effect relationship. *Cancer Res.* 4664–4669
107 Scott, A.M. *et al.* (2012) Antibody therapy of cancer. *Nat. Rev. Cancer* 12, 278–287
108 Di Gaetano, N. *et al.* (2003) Complement activation determines the therapeutic activity of rituximab *in vivo*. *J. Immunol* 171, 1581–1587
109 Golay, J. *et al.* (2006) The role of complement in the therapeutic activity of rituximab in a murine B lymphoma model homing in lymph nodes. *Haematologica* 91, 176–183
110 Beckman, R. *et al.* (2007) Antibody constructs in cancer therapy: protein engineering strategies to improve exposure in solid tumors. *Cancer* 109, 170–179
111 Holliger, P. and Hudson, P.J. (2008) Engineered antibody fragments and the rise of single domains. *Nat. Biotechnol* 23, 1126–1136
112 Aires da Silva, F. *et al.* (2008) Recombinant antibodies as therapeutic agents. *BioDrugs* 22, 301–314
113 Hamers-Casterman, C. *et al.* (1993) Naturally occurring antibodies devoid of light chains. *Nature* 363, 446–448
114 Muyldermans, S. (2001) Single domain camel antibodies: current status. *J. Biotechnol.* 74, 277–302
115 Pares, S. and Mouz, N. (1996) The crystal structure of a llama heavy chain variable domain. *Nat. Struct. Biol.* 3, 752–757
116 Muyldermans, S. and Lauwereys, M. (1999) Unique single- domain antigen binding fragments derived from naturally occurring camel heavy-chain. *J. Mol. Recognit* 131–140
117 Steeland, S. *et al.* (2016) Nanobodies as therapeutics: Big opportunities for small antibodies. *Drug Discov Today* 21, 1076–1113
118 Bell, A. *et al.* (2010) Differential tumor-targeting abilities of three single-domain antibody formats. *Cancer Lett.* 289, 81–90
119 Tang, Z. *et al.* (2013) A human single-domain antibody elicits potent antitumor activity by targeting an epitope in mesothelin close to the cancer cell surface. *Mol. Cancer Ther.* 12, 416–426
120 Fogal, V. *et al.* (2009) Cell surface nucleolin antagonist causes endothelial cell apoptosis and normalization of tumor vasculature. *Angiogenesis* 12, 91–100
121 Sutkowski, N. *et al.* MUSC Foundation for Research Development. Human monoclonal antibodies to human nucleolin. US Pat.20160215050.
122 Fernandes, D.J. *et al.* (2016) Development of anti-nucleolin antibodies with broad spectrum anticancer activity and negligible toxicity to normal cells. *Cancer Res.* 76 (Suppl), 1488
123 Palmieri, D. *et al.* (2015) Human anti-nucleolin recombinant immunoagent for cancer therapy. *Proc. Natl. Acad. Sci. U. S. A.* 112, 9418–9423
124 D'Avino, C. *et al.* (2016) A novel fully human anti-NCL immunoRNase for triple-negative breast cancer therapy. *Oncotarget* 7, 87016–87030
125 Romano, S. *et al.* (2018) Anticancer activity and antibody-dependent cell-mediated cytotoxicity of novel anti-nucleolin antibodies. *Sci. Rep.* 8, 7450

126 Aravind, A. *et al.* (2012) AS1411 aptamer tagged PLGA-lecithin-PEG nanoparticles for tumor cell targeting and drug delivery. *Biotechnol. Bioeng.* 109, 2920–2931
127 Liao, Z.X. *et al.* (2015) An AS1411 aptamer-conjugated liposomal system containing a bubble-generating agent for tumor-specific chemotherapy that overcomes multidrug resistance. *J. Control. Release* 208, 42–51
128 Zhuang, Y. *et al.* (2016) Aptamer-functionalized and backbone redox-responsive hyperbranched polymer for targeted drug delivery in cancer therapy. *Biomacromolecules* 17, 2050–2062
129 Alibolandi, M. *et al.* (2016) AS1411 aptamer-decorated biodegradable polyethylene glycol-poly(lactic-co-glycolic acid) nanopolymersomes for the targeted delivery of gemcitabine to non-small cell lung cancer *in vitro*. *J. Pharm Sci.* 105, 1741–1750
130 Chen, Z. *et al.* (2016) Aptamer-mediated delivery of docetaxel to prostate cancer through polymeric nanoparticles for enhancement of antitumor efficacy. *Eur. J. Pharm. Biopharm.* 107, 130–141
131 Tao, W. *et al.* (2016) Polydopamine-based surface modification of novel nanoparticle-aptamer bioconjugates for *in vivo* breast cancer targeting and enhanced therapeutic effects. *Theranostics* 6, 470–484
132 Xu, G. *et al.* (2016) Robust aptamer-polydopamine-functionalized M-PLGA-TPGS nanoparticles for targeted delivery of docetaxel and enhanced cervical cancer therapy. *Int. J. Cancer* 11, 2953–2965
133 Alibolandi, M. *et al.* (2017) Smart AS1411-aptamer conjugated pegylated PAMAM dendrimer for the superior delivery of camptothecin to colon adenocarcinoma *in vitro* and *in vivo*. *Int. J. Pharm.* 519, 352–364
134 Wang, Y. *et al.* (2017) Nucleolin-targeted extracellular vesicles as a versatile platform for biologics delivery to breast cancer. *Theranostics* 7, 1360–1372
135 Mosafer, J. *et al.* (2017) *In vitro* and *in vivo* evaluation of anti-nucleolin-targeted magnetic PLGA nanoparticles loaded with doxorubicin as a theranostic agent for enhanced targeted cancer imaging and therapy. *Eur. J. Pharm. Biopharm.* 113, 60–74
136 Zhang, R. *et al.* (2017) Co-delivery of doxorubicin and AS1411 aptamer by poly (ethylene glycol)-poly(β-amino esters) polymeric micelles for targeted cancer therapy. *J. Nanoparticle Res.* 19, 224
137 Krust, B. *et al.* (2011) Suppression of tumorigenicity of rhabdoid tumor derived G401 cells by the multivalent HB-19 pseudopeptide that targets surface nucleolin. *Biochimie* 93, 426–433